Statistical Mechanics of Clogging

I. Zuriguel and A. Garcimartín
Dpto. de Física y Mat. Apl. Facultad de Ciencias, Universidad de Navarra, Pamplona, Spain

Article Outline

Glossary

Arch Set of mutually stabilizing particles, meaning that if any one of them is removed the whole set will collapse.

Clogging Halt of the flow of macroscopic particles caused by the development of a local structure (an arch in two dimensions or a dome in three) which brings the whole system to a rest state.

Granular matter Material composed of independent, macroscopic particles that interact solely by contacts or collisions. As the latter are intrinsically dissipative, energy is not conserved, and therefore, the system typically adopts metastable configurations.

Granular Silo Container in which granular matter is stored. The emptying of silos is generally performed through an orifice at the bottom, although other alternatives (such as the discharge through lateral orifices or by means of extraction belts) are also possible.

Unclogging Destabilization of a clogging arch by means of an energy input which must be external for the case of inert granular media, but can be also internal for other systems such as active matter.

Definition of the Subject

Clogging is defined as an arrest of the flow of macroscopic particles caused by the formation of a local arrangement that is generally metastable. Usually, clogging occurs at bottlenecks when the neck-to-particle size ratio is slightly above the unity. Although clogs may appear in a wide variety of systems – such as cells, colloids, or live beings – we will focus here on clogging in granular matter as a prototypical and simple case. Understanding clogging in granular systems is important from the industrial and environmental viewpoint. Indeed, clogging in silos or hoppers may completely halt a production line in food or pharmaceutical industries. Also, a safe and efficient handling of raw materials in mining is important to prevent environmental harm and to reduce production costs. But even in granular matter, understanding clogging poses a tough challenge as the arch formation is essentially a local phenomenon that drives the whole system to a sudden arrest. Contrary to other physical processes like jamming, the definition of average magnitudes – such as volume fraction, for instance – is not straightforward.

Clogging is intimately related to the formation of arches and their stability. Therefore, introducing an excitation at the outlet or nearby can be a suitable strategy to destroy the clog and resume the flow. Thus, when a vibration is applied at the bottom of a silo, the flow may become intermittent resembling the dynamics observed in other active systems flowing through constrictions. The phys-

R. A. Meyers (ed.), *Encyclopedia of Complexity and Systems Science*,
https://doi.org/10.1007/978-3-642-27737-5_746-1

ics underlying clogging, on one side, and unclogging, on the other side, is not the same, as revealed by the different nature of their statistical properties. In the following sections we will deep into this question and others, such as the arguments on the existence or not of a critical outlet size above which clogging is not possible, a subject discussed since mid last century.

Introduction

The dense flow of granular materials through a narrowing is a complex situation. At the bottleneck, the system undergoes a transition from fluid like behavior (above the opening) to gas like behavior (after the neck, where the contacts among particles are sparse). This flow becomes even more complicated when the aperture is only a few times larger than the typical particle size; in this scenario there exists the possibility that a metastable structure forms spanning the whole outlet, causing a complete arrest of the grains.

Although by the end of the last century an abundant number of devices were created – and even patented – to prevent clogging, the problem fundamentals were only scarcely studied at that time. As a matter of fact, most of the works were aimed at determining the size of the outlet that guaranteed a continuous flow through the silo outlet (Arnold and McLean 1976; Drescher et al. 1995; Jenike 1964; Walker 1966). Conversely, there was a remarkable interest on investigating the flow properties in the silo discharge; the focus was mostly put on the flow rate dependence on the outlet size (Beverloo et al. 1961). In most cases, the orifices were large enough to prevent clogging, which was considered as an aside problem to be avoided. Indeed, from an applied point of view, clogging avoidance was the main concern at that time and this is reflected on the focus of the investigations that were performed.

In the last two decades, the study of clogging in granular silos has regained the attention of the scientific community. Among others, two reasons may be pointed out for this appealing. First, clogging is an apparently simple everyday problem (we all have to shake the saltcellar to pour salt in our food) with a fundamental interest, where deep questions arise, and it is accessible to researchers with limited resources. Second, given the inert nature of the grains, clogging in silos has been taken as a standard against which to compare clogging in other, more complex systems. As examples, we pinpoint the flow through bottlenecks of colloids, microbial populations, mechanically self-driven robots, suspensions, pedestrians, animals, and other kinds of active matter. Given the different nature of the particles composing these systems, it becomes obvious that the analogies are only qualitative; despite this, some of the models and analytical approaches introduced for the granular case can be used as a starting point for more sophisticated elaborations pertinent to those other systems.

Remarkably, the number of applications in which clogging is a paramount concern is much larger if all these related many-body systems are included. For example, clogging of a dense microparticle suspension can occlude microchannel constrictions, a behavior that is exploited in medicine to provoke embolization of blood vessels in order to shrink a tumor. Besides, the formation of clogs in suspensions of larger particles is crucial in determining the lifetime of subsurface flow treatments, a widely used alternative to remove pollutants from wastewater. Similarly, clogging of suspended hydrated particles is a major issue concerning oil and gas transport through pipelines. A reasonable understanding of clogging is also necessary to guarantee a good performance of slit-structures, which are rigid barriers with one or more slits built in craggy mountains to reduce avalanche hazard. Last but not least, clogging has also occasionally happened in crowds trying to evacuate enclosed areas in highly competitive and dire situations.

In all the examples given above, a geometrical constriction (i.e., a bottleneck) is at play. However, it has been recently shown that this specific geometry is not imperative to observe clogging. Indeed, if the particles are sufficiently confined, a blockage may also show up in a straight channel. This happens for instance in underground mining, where raw materials driven by gravity are conveyed through vertical pipes from one level of the

mine to another. In this case, the blocking arches do not rest on the silo bottom or hopper walls, but lean against the vertical walls of the pipe. This is possible due to frictional forces, and the effect is magnified because of the geometrical frustration introduced by the flat faceted stones that are typically transported in these channels. Although here we will focus on the bottleneck geometry, several works about clogging in straight channels and obstacle arrays – an interesting configuration that may turn out to be useful for linking clogging and jamming behavior – will also be described.

Clogging

Clogging as a Stochastic Process

Let us consider a container full of grains discharged through an orifice at the bottom which is only a few times larger than the typical particle size. In this scenario, the probability that a clogging arch develops is constant over time, that is, it is a Poisson process. This fact implies that:

1. There is no way to predict exactly when the system will get clogged.
2. Clogging is a history independent process: even if the system has been flowing for a lot of time, the probability of getting clogged remains the same.
3. If we define the avalanche size as the number of grains flowing out the silo before an arch clogs it, the distribution of these sizes will follow an exponential tail.
4. There is no correlation among the size of consecutive avalanches.
5. The average avalanche size is well defined.

The first evidence of the exponential nature of the avalanche size distribution was reported by Clément et al. (2000) as shown in Fig. 1. Subsequently, Zuriguel et al. corroborated this feature and provided an interpretation in terms of a probabilistic model (Zuriguel et al. 2003). The idea was to assign the same probability of clogging p_c to all particles inside the silo. Therefore, the probability that a particle passes through the outlet without forming a clog can be written as $p_p = 1 - p_c$, and the probability of getting an avalanche of s particles can be described by Eq. 1 (note that the original equation proposed was $n(s) = p_p^s p_c^2$ as it was considered also the precedent clogging event but it was posteriorly (Zuriguel et al. 2005) corrected to Eq. 1).

$$n(s) = p_p^s p_c \tag{1}$$

That is, the probability of getting an avalanche of size s is obtained by multiplying s times the probability that a particle passes through the exit and one time the probability that the particle clogs it. This definition allows a straightforward connection between the first moment of the distribution (the mean avalanche size) and p_c (Janda et al. 2008):

$$\langle s \rangle = \frac{p_p}{p_c} \tag{2}$$

In most of the scenarios investigated the avalanches are larger than about 100 particles. In this case $p_p \simeq 1$, and therefore $\langle s \rangle \simeq p_c^{-1}$.

Another salient feature reported in Zuriguel et al. (2003) was the apparent lack of correlation among the size of consecutive avalanches (see Fig. 2). If we accept the hypothesis of lack of memory in the passage of particles within a single avalanche, it is not surprising that the statistics of consecutive avalanches are independent.

Although the probabilistic model leading to Eq. 1 was obtained by assigning to each particle a given probability of forming a clog, the same reasoning is valid if groups of particles are considered instead, as stated in Zuriguel et al. (2003). Indeed, it is obvious that the development of a clogging arch is a process involving several particles. In order to account for this issue, Masuda et al. (2014) devised a model in which the arch formation region was split into discrete sites that can contain at most one particle. By defining a particle inflow rate α and different outflow rates depending on the occupancy of neighboring sites (see Fig. 3), different dynamics were observed including flow intermittency and clog formation. The later occurred when all sites were filled.

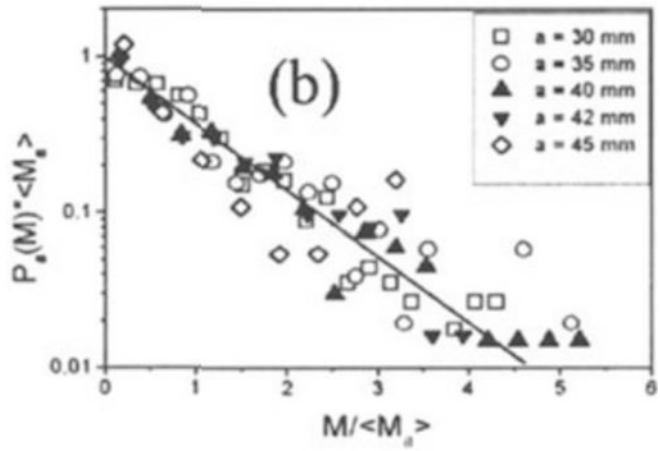

Statistical Mechanics of Clogging, Fig. 1 Rescaled mass distributions of avalanches for different outlet sizes a, as indicated in the legend. $P_a(M)$ is the probability density for an avalanche with mass M for an outlet size a. The average avalanche mass is $\langle M_a \rangle$. The solid line displays an exponential decay. (Reprinted from Clément et al. (2000))

Remarkably, this model recovers the exponential distribution of avalanche sizes.

A similar approach of dividing the space in cells was in fact implemented a decade before by Helbing and coworkers in a work (Helbing et al. 2006) where they presented an analytical model which served for both granular bottleneck flows and pedestrian escape dynamics through a narrowing. Based on a continuity equation in polar coordinates, they observed shockwaves when the inflow exceeds the maximum outflow. More importantly for the case we are analyzing here, their model gave rise to three different regimes depending on the exit size: no flow for small exits, intermittent flow for medium size doors, and continuous flow for large enough openings. In the intermittent flow scenario, exponentially distributed avalanche sizes were reported in good agreement with experimental data.

Up to now, we have described several works where the exponential distribution of avalanche sizes is observed and explained in different, but similar, ways. All share the idea that clogging is a stochastic process where the probability of a clog depends on the outlet size, as will be explained below. The exponential distribution of avalanches is considered as a hallmark of the flow of discrete particles through bottlenecks and has been also reproduced by many authors in different geometries and scenarios (Kondic 2014; Pérez 2008; Sheldon and Durian 2010). Nevertheless, there is an exception to this accepted rule: when the orifice is strongly asymmetric the avalanche statistics resemble more a power law than an exponential distribution. This was discovered by Saraf and Franklin when working with wedge hoppers having an orifice that was around 20 times longer than wider (Saraf and Franklin 2011). The explanation given for this feature assumed that the clogging probability of strings of particles depends on their orientation. By considering a uniform distribution of probabilities and integrating over all the allowable string orientations, an expression is obtained for the avalanche size distribution that depends on the exit geometry. In particular, the well-known exponential distribution is generated for isometric (round) orifices, whereas for anisometric exits the expression tends to an asymptotic value that scales as $n(s) \sim s^{-2}$.

Does a Critical Outlet Size Exist?

The supply of a continuous flow of grains through the orifice (i.e., preventing clog formation) was the ambition of the pioneering engineers who studied silo clogging. For this reason, the research since the 1960s has been primarily focused in finding the outlet size that guaranteed a complete absence of clogging (Arnold and McLean 1976; Drescher et al. 1995; Jenike 1964; Walker 1966). The approach followed in these works was to set up the stress-strain rate relations and analyze the critical factors which ensured continuous gravity flow. From this, a typical orifice value of around 5 to 10 times the particle size was found for non-cohesive grains.

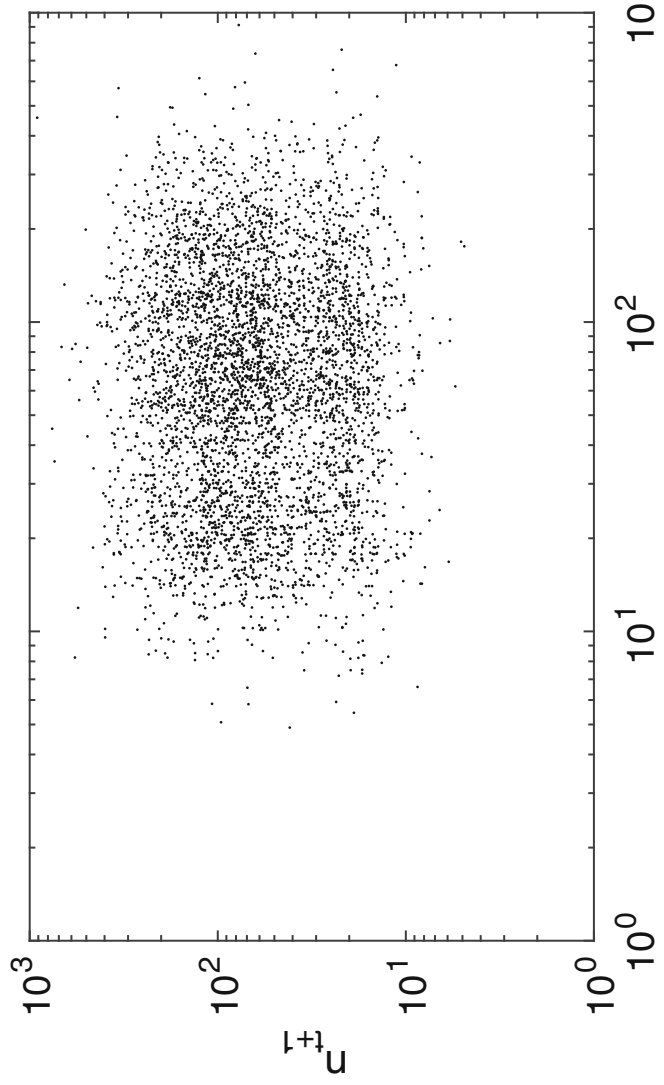

Statistical Mechanics of Clogging, Fig. 2 First return map of avalanche sizes, that is, the avalanche size $n_t + 1$ vs. the previous avalanche size n_t, where t is a correlative index ordering the sequence of avalanches. (Reprinted from Zuriguel et al. (2003))

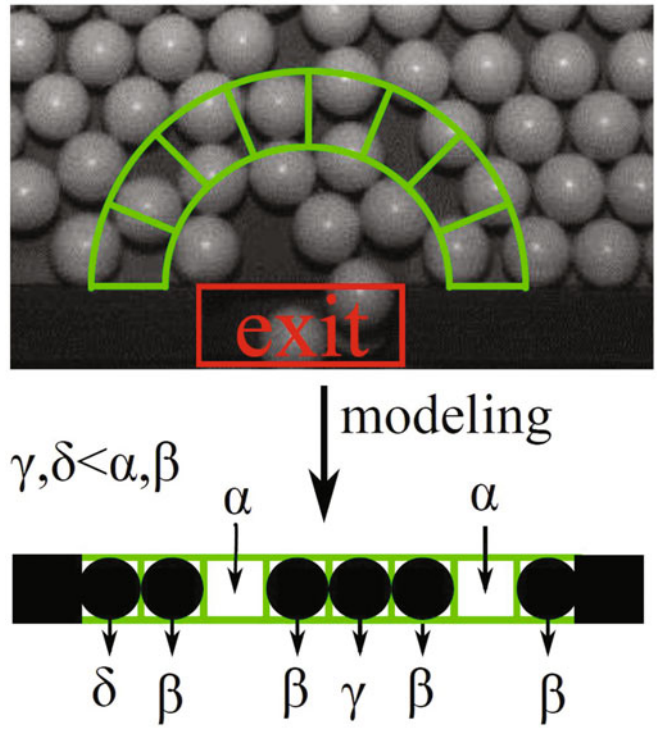

Statistical Mechanics of Clogging, Fig. 3 Arch formation model in which the arch region is divided in several cells of about the size of a particle (top). In the bottom, one-dimensional projection of the arch where arrows into a site represent a particle "inflow" at a rate α. The arrows pointing out of sites indicate the "outflow" which is defined by three-site interactions. When a filled site is besides an empty site, the outflow rate is defined by β. When a filled cell is surrounded by two filled cells, the outflow rate is γ; and when a filled cell is between a filled cell and a boundary, the outflow rate is δ. (Reprinted from Masuda et al. (2014))

Instead, modern approaches involve statistical analysis of the avalanche sizes or clogging probability, and their dependence on the outlet size. In the following subsection we summarize some recent advances in this area.

Statistics of Avalanches

In their trailblazing work K. To et al. (2001) measured a quantity they called J – the probability that a two-dimensional silo filled with a fixed number of grains gets jammed before emptied – for different outlet sizes (Fig. 4). The most salient feature they observed was a strong dependence of J on the outlet size, which suggested a transition to a state where $J = 0$ (i.e., complete absence of clogging) for an opening size of around 5 to 7 particle diameters. In order to describe this transition, the authors developed a model in which the clogging arch was envisaged as a restricted random walker. In this model, the particles conforming the arch took random positions with some restrictions:

1. The random walker goes from left to right.
2. The arch has to be convex at all sites to guarantee its stability.
3. The particles cannot interpenetrate each other.
4. The total span of the arch has to be larger than the outlet size.

This model successfully described the jamming probability dependence on the outlet size for the experimental conditions implemented in that work, showing values of J tending to zero for large enough outlet sizes. However, the question about the existence of a transition (in the thermodynamic sense) from a jammed state to an unjammed one remained open.

This problem was approached by Zuriguel et al. (2005), who used a three-dimensional silo to experimentally investigate the clogging probability in a wide range of outlet sizes, including some cases with a very low probability of clogging. Remarkably, they explored outlet sizes in which the mean avalanche size was above 10^6

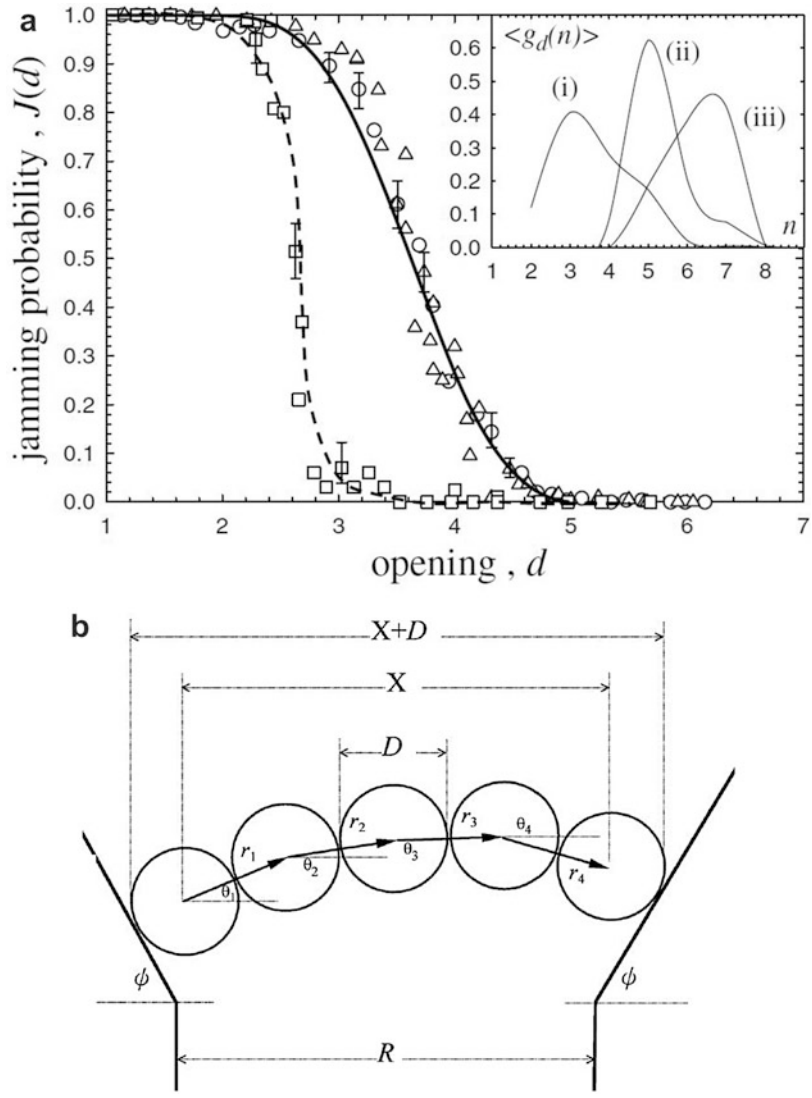

Statistical Mechanics of Clogging, Fig. 4 Left: probability that a silo gets jammed J versus the outlet size. Data correspond to hoppers of different angles ϕ: circles ($\phi = 34°$), triangles ($\phi = 60°$), and squares ($\phi = 75°$). Right: Sketch of an arch clogging a hopper of angle ϕ with an exit size R. The angles among consecutive particles are defined, from left to right, as θ_1, θ_2,... θ_{n-1}. (Reprinted from To et al. (2001))

particles and proposed Eq. 3 as the best fitting expression for their data. As it is evidenced in Fig. 5, the fitting was quite good with the following parameter values: $\gamma = 6.9 \pm 0.2$, $A = 9900 \pm 100$, and $R_c = 4.94 \pm 0.03$. Notably, the figure obtained for the critical outlet size was similar to previous predictions based on the stress-strain rate relations reported at the end of the twentieth century. The unusually high value of the exponent, apart from manifesting the strong dependence of the avalanche size on the outlet size, also hinted to the need of looking for another order parameter (instead of the avalanche size) that better describes the clogging transition. In addition, it was shown that R – the outlet size rescaled by the particle diameter – is the most important parameter on determining the clogging probability. In fact, experiments with different outlet sizes and particle diameters, but the same R, displayed very similar results (Fig. 5, right). Also, the effect on clogging of the material properties of the particles was revealed to be rather small.

$$\langle s \rangle = \frac{A}{(R_c - R)^{\gamma}} \tag{3}$$

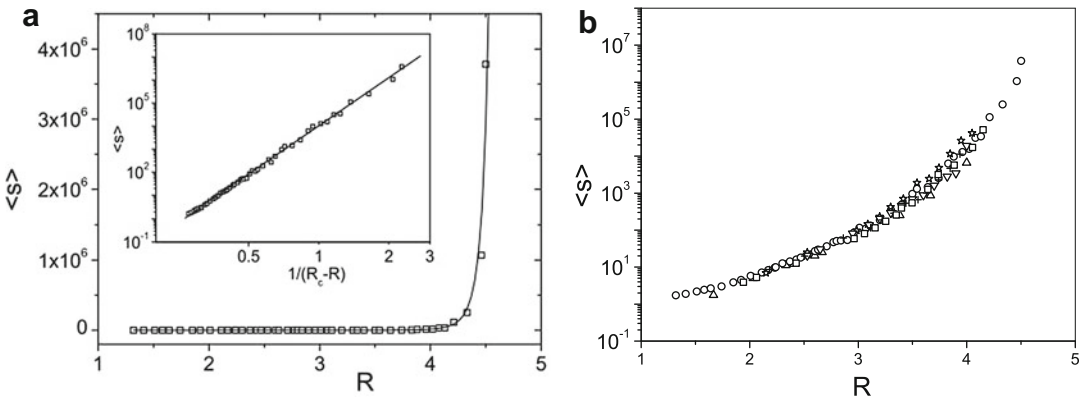

Statistical Mechanics of Clogging, Fig. 5 Left: mean avalanche size versus the exit size R. In the inset, mean avalanche size versus $(R_c - R)^{-1}$ in logarithmic scale. In both cases the fit corresponds to Eq. 3 with the parameters indicated in the text. Right: mean avalanche size vs R in a semilogarithmic scale; data correspond to spherical grains of different materials (delrin, glass, lead, and steel) and different particle diameters (from 1 to 3 mm). (Reprinted from Zuriguel et al. (2005))

Shortly after the introduction of this power law fit, K. To suggested that two other expressions were able to fit the data equally well (at least for experiments in two-dimensional silos) (To 2005). One of such expressions (Eq. 4) was a stretched exponential which did not involve a critical outlet size. Later on, this result was given additional support by Janda et al. (2008) for the two-dimensional case, a scenario for which the origin of the equation was related with the statistics of the arch lengths obtained in static deposits of grains. Nevertheless, the goodness of Eq. 4 to fit the outcomes of a three-dimensional silo was challenged, suggesting that the fitting was neither satisfactory when raising R to a power of 3 (the dimension of the system).

$$\langle s \rangle = A\, e^{B R^2} \tag{4}$$

Following another line of reasoning, Thomas and Durian (2015) build upon experimental data of avalanche sizes in a wide variety of situations (hoppers with several tilt angles, orifices with different geometries, particles of diverse nature, and so on) to show that the three fitting expressions proposed by K. To worked nicely in three dimensions (Fig. 6). Moreover, the origin of the $\langle s \rangle = Ae^{B R^3}$ relationship was justified by considering all possible arch configurations and evaluating the amount of them that would be effectively able to block the orifice. The same approach was afterwards further elaborated by researchers of the same group (Koivisto and Durian 2017) to successfully evaluate the effect of interstitial fluid on the clogging probability.

Dynamical Signatures of Clogging

An alternative way of approaching the question of whether there is a critical outlet size above which clogging would never happen is to look for dynamical flow features that could reveal any difference at both sides of the hypothetical transition point. The first proof of the existence of such differences was reported by Longhi et al. (2002) in a work where they characterize the impulses delivered to the wall of a 2D hopper. They found that the distribution of impulses decayed exponentially for impulses above the average, in the same way that the forces in a static granular packing do (Mueth et al. 1998). This happens independently on the hopper size, which only affects the impulse distribution for values below the average. However, these small impulses display a smooth evolution when going from continuous to intermittently jamming flows; so there was not any signature of a proper clogging transition. Nevertheless, as reported in the same work, the

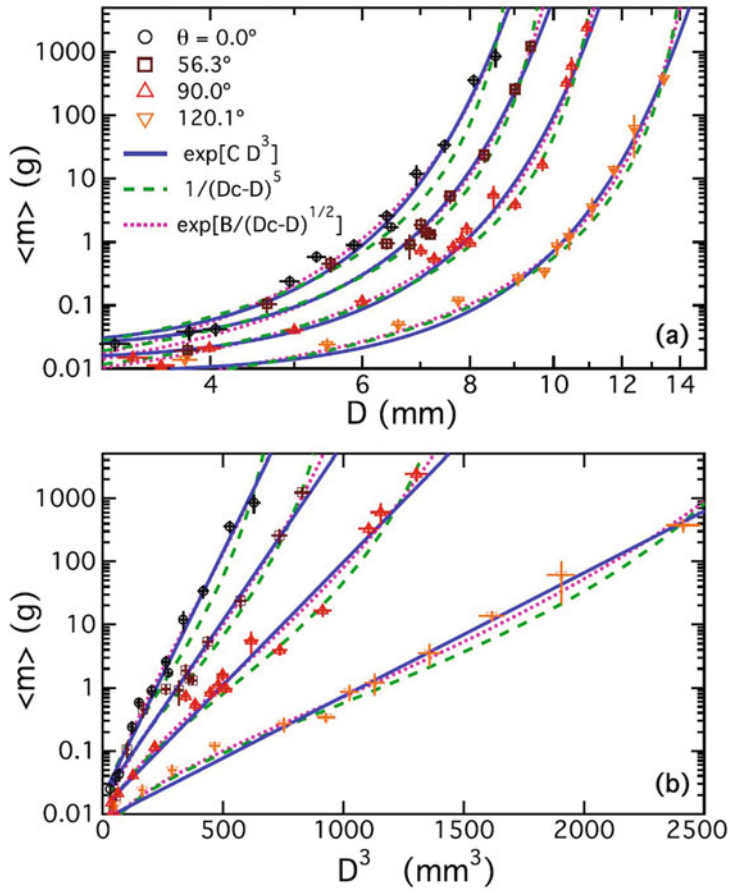

Statistical Mechanics of Clogging, Fig. 6 Left: mean avalanche size (in grams) versus the exit size. Data for hopers with different tilt angles as indicated in the legend. The three line types represent different fitting alternatives. Right: the same data and fits using the outlet size raised to the third power in the abscissa axis. (Reprinted from Thomas and Durian (2015))

distributions of time intervals among consecutive collisions did hint an approach to jamming as they tend to a power law distribution with an exponent $-3/2$ when the outlet size was progressively reduced (see Fig. 7).

An additional signature of clogging has been identified by analyzing the fluctuations of the flow rate. In this regard, Janda et al. (2009a) implemented high-speed video recordings to detect the passage of every individual grain through the outlet. With this information the flow rate was calculated in very short temporal windows (of the order of 0.1 s) for different outlet sizes. Interestingly, the distributions of the instantaneous flow rate q were Gaussian for large outlet sizes (where clogging never happens), whereas they became strongly asymmetric for small outlet sizes (where clogging eventually occurs). In the latter case, a strong increase of the number of events toward small values of q was found, displaying a peak at $q = 0$ that was related with the formation of unstable clogs (see Fig. 8). Therefore, a relationship between the appearance of unstable clogs and stable ones was established, and it was suggested that the total absence of unstable clogs for large outlet sizes was reflecting the existence of a "clogging free" region.

A similar increasing of the fluctuations when reducing the outlet size was reported by Thomas and Durian (2016). In particular, they measured the relative velocity fluctuations and the skewness of the velocity distribution. They also quantified the intermittency by means of a descriptor based on the two-sample Kolmogorov-Smirnov statistic. All these estimators were shown to grow for flows more prone to clogging, that is, when the outlet size was reduced. However, the evolution of these magnitudes with R was smooth

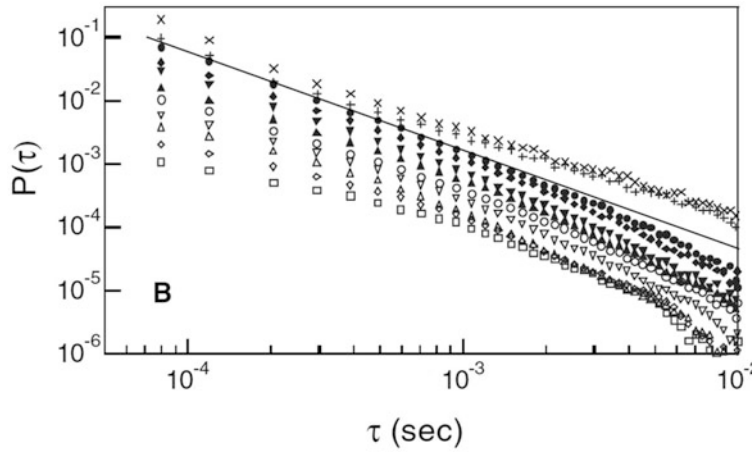

Statistical Mechanics of Clogging, Fig. 7 Logarithmic plot of the probability distributions $P(\tau)$ of the time intervals τ between collisions, for opening sizes ranging from $R = 3$ (top series) to $R = 16$ (bottom). (Reprinted from Longhi et al. (2002))

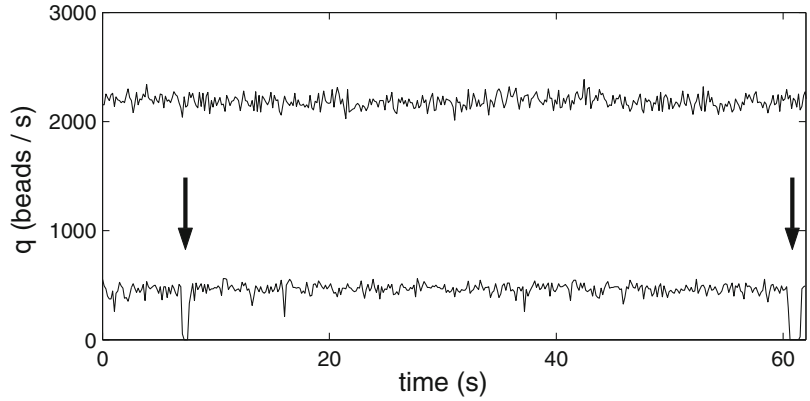

Statistical Mechanics of Clogging, Fig. 8 Instantaneous flow rate (in number of particles per unit time) measured at short time windows (of 150 ms). The line at the top corresponds to an orifice size of $R = 9.5$, and the one at the bottom to an orifice of $R = 4.3$. The arrows mark two events where the flow has ceased for a time longer than the window. (Reprinted from Janda et al. (2009a))

and no discontinuity or kink was observed for a hypothetical critical outlet size. Therefore, this analysis undermined the hypothesis of a critical outlet size, supporting instead the notion that clogging is always possible, irrespective of the outlet size.

Incipient Clogging Let us finally mention here a couple of works where different dynamical signatures of incipient clog formation were reported. In 1993, Sakaguchi et al. (1993) suggested that the flow in a 2D silo with a small orifice consisted on an alternation of flows coming from both sides of the outlet. At the instant when the transition (flow from one side to flow from the other side) occurred, the grains collided, thus facilitating the formation of the arches that would lead to clogging. Alternatively, Tewari et al. (2013) performed numerical simulations of silo discharge and gridded the space into a number of boxes in which the vertical velocity was calculated. Then, the boxes with an instantaneous velocity below half the average were assigned to clusters. From these data, it was observed that just before the appearance of a clog, there was a notable increase of the area covered by these clusters comprising regions with a markedly low velocity. In the same way, after the flow was resumed, the area of these clusters decreased, as

displayed in Fig. 9. Moreover, clog formation was associated to the development of vortices at the corners of the hopper that extended inwards, eventually arresting the flow.

Effect of Other Variables

Clearly, the parameter that mainly determines the clogging probability (and hence, the avalanche size) is the ratio R among the outlet and the particle size. As displayed above (Fig. 5b), its effect is so important that an increase from $R = 3$ to $R = 4$ leads to a growth of the avalanche size by more than 100 times. Due to this dramatic dependence, the main way to analyze the influence of other variables has been to keep a strictly constant outlet size (sometimes a variation of a tenth of millimeter may conceal the effect of other quantities). A time-consuming alternative consists of repeating a series of experiments for all the range of outlet sizes changing an additional parameter.

The latter was, indeed, the strategy followed by K. To and collaborators to analyze the role of the hopper angle (To et al. 2001). Oddly enough, they observed that for small and medium hopper angles (close to a flat bottomed silo) this parameter had a negligible effect on the probability of clogging ($\phi = 34^\circ$ and $\phi = 60^\circ$ displayed almost the same values). Nevertheless, clogging was dramatically reduced when using a hopper of $\phi = 75^\circ$. This strongly nonlinear dependence has been recently confirmed and explained by considering the angles among the particles conforming the arch (López-Rodríguez et al. 2019) in a two-dimensional silo. This approach revealed that increasing the hopper angle extended the number of forbidden arch configurations, that is, those that would imply interparticle angles that could not be stabilized with typical friction forces. Although this interpretation has not been yet extrapolated to three-dimensional silos, recent results reported in Parretta and Grillo (2019) are perfectly compatible with it. In Arches (devoted to the geometry of clogging arches) we will come back to the role of particle angles in the arch stability.

A similar line of reasoning could be valid to deal with clogging in lateral and inclined orifices. In two manuscripts from Durian's group (Sheldon and Durian 2010; Thomas and Durian 2013), a clogging phase diagram was suggested when considering its dependence on two parameters: the outlet size and the tilt angle of the silo (Fig. 10). Remark that it is tempting to consider silo tilt as a situation similar to using different hopper angles, but there are conspicuous differences. For instance, it was reported that for a given outlet size the clogging probability grows when increasing the tilt angle (opposite to the hopper case). Moreover, by implementing experiments in both, symmetric orifices (circular) and asymmetric ones (slits), these authors showed that the behavior in all these systems could be encompassed by using the projected area of the aperture over the average flow direction (instead of the gravity direction) as depicted in Fig. 10. In principle, this collapse of the transition points should be also valid for completely vertical orifices, a scenario where the wall width is capital (Davies and Desai 2008; Serrano et al. 2014; Zhou et al. 2017).

Certainly, one of the most surprising features concerning clogging appears when an obstacle is placed above the orifice (Lozano et al. 2012a; Zuriguel et al. 2011). This geometrical constraint, which a priori would restrict the flow of grains, turns to be beneficial if the obstacle position is carefully selected. Indeed, the effect can be utterly remarkable, as in some cases the avalanche size is increased by more than one hundred times. The physical origin of this behavior was speculated to be related with the arch stabilization process. According to this argument, in a usual silo without an obstacle, a stable arch can develop when a group of particles collides above the orifice due to the confinement imposed by the particles coming from above. On the contrary, for some obstacle positions, there is an effective reduction of pressure above the orifice that allows the colliding particles to be ejected upwards, thus preventing the formation of a stable arch. A demonstration of this behavior was numerically given in Zuriguel et al. (2011) by simulating clogging in silos filled with thin layers of grains. In fact, reducing the height of the granular column inside the silo caused an increase of the mean avalanche size comparable to the one obtained when placing the obstacle. In addition, in Lozano et al. (2012a) it

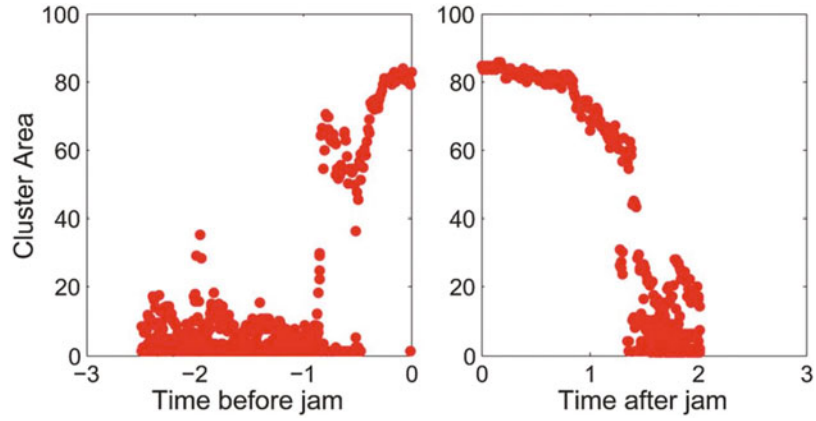

Statistical Mechanics of Clogging, Fig. 9 Temporal evolution of the area covered by connected clusters of low velocity regions (where the vertical velocity is less than half the average) near the orifice. As it can be seen, the area starts growing before the formation of a clog and decreases when the flow is resumed. (Reprinted from Tewari et al. (2013))

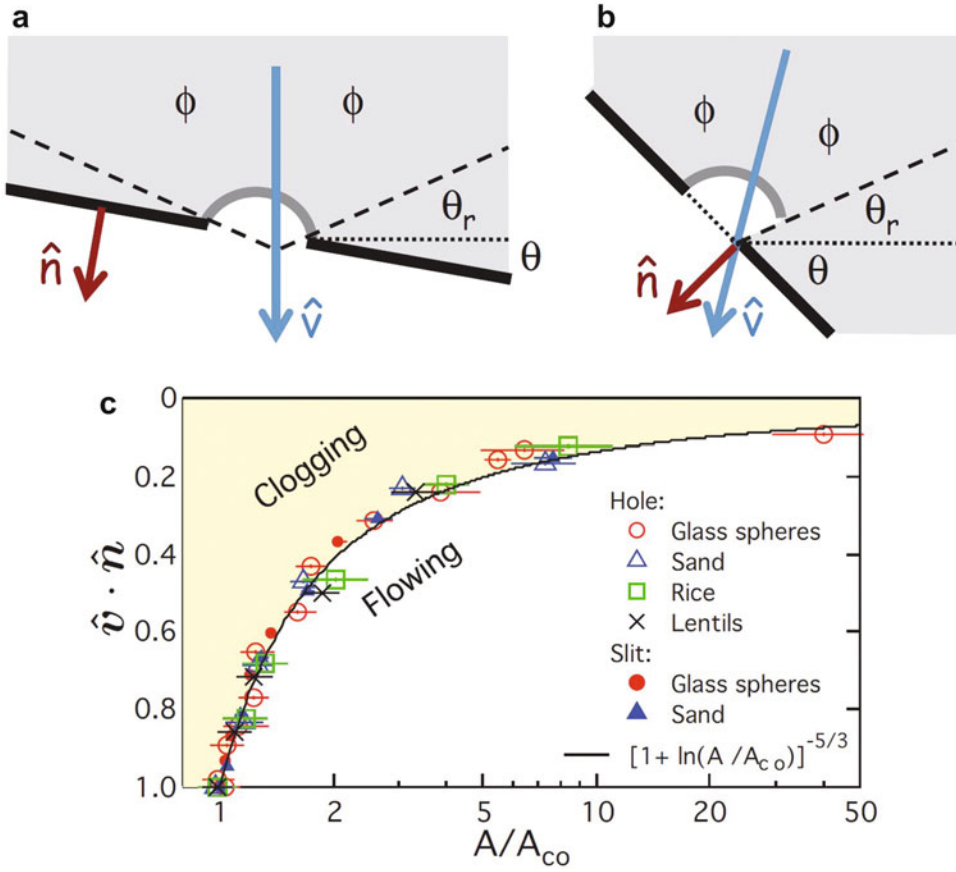

Statistical Mechanics of Clogging, Fig. 10 Top: sketch of the orifice indicating the unit vectors $\hat{n}$ (normal to the plane of the aperture) and $\hat{v}$ (average flow direction, as defined by bisecting the region where the grains flow) when the tilt angle θ is (a) less than, and (b) greater than, the angle of repose θ_r. Bottom: Clogging transition diagram for holes and slits and different types of particles. The y-axis is the component $\hat{v} \cdot \hat{n}$ of the unit vectors defined above and the x-axis is the area of the hole normalized by the critical hole area at zero tilt angle. (Reprinted from Thomas and Durian (2013))

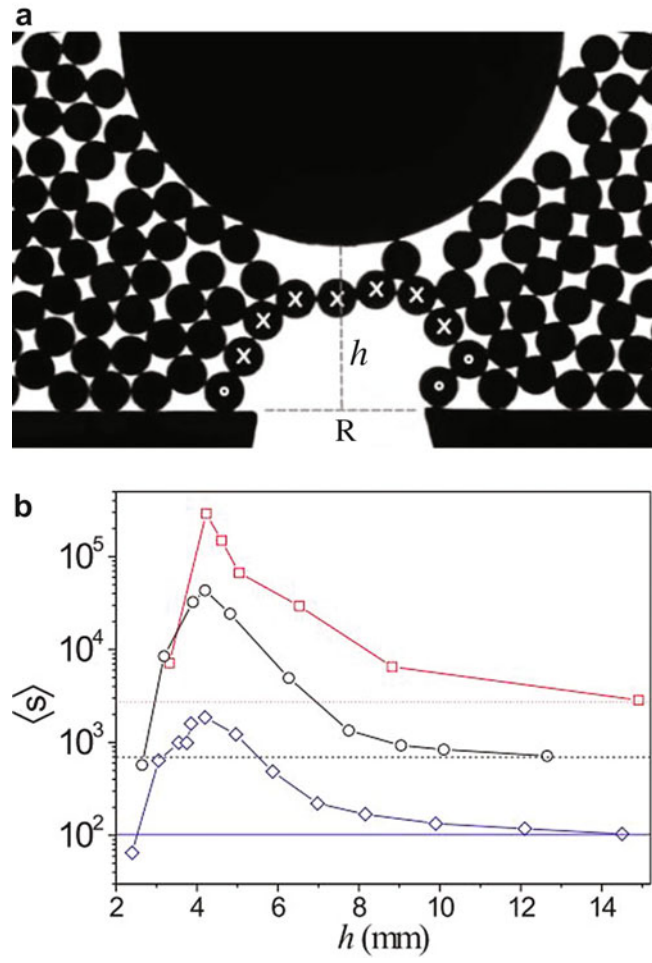

Statistical Mechanics of Clogging, Fig. 11 Left: photograph of an arch formed above the outlet. R is the length (or size) of the outlet and h is the distance from the bottom of the obstacle to the outlet. Right: mean avalanche size versus the obstacle position for silos with three different outlet sizes (from bottom to top: $R = 3.13$, $R = 4.20$ and $R = 4.55$). The horizontal lines correspond to the mean avalanche size without obstacle for each outlet size. (Reprinted from Lozano et al. (2012a))

was shown that the clogging reduction effect increased when enlarging the outlet size (see Fig. 11). This can be understood if we consider that the system becomes more sensitive to perturbations when approaching the hypothetical critical outlet size. Although these features were originally reported using a circular obstacle, other authors have implemented different shapes, such as triangular, inverted-triangular, and a horizontal bar (Endo et al. 2017). Among these forms, the triangular obstacle and the horizontal bar were shown to be the most effective to prevent clogging. These authors also attribute the clogging reduction to a decrease in the packing fraction at the exit region. Even though this justification seems different from the pressure reduction explained above, it should be noted that both variables are strongly coupled in granular materials.

Implementing multiple orifices in a silo appears as a natural extension of previous investigations with a single orifice (Kunte et al. 2014; Mondal and Sharma 2014). In this system, if two orifices are sufficiently close to each other, it is possible to obtain an intermittent flow. The reason is that if an arch blocks only one of the orifices, the flow through the other one can cause the destabilization of the former and restart the flow through it. This behavior has been observed in three- (Mondal and Sharma 2014) and two-dimensional silos (Kunte et al. 2014) and can be used to reduce the overall clogging probability. As could be expected, the distance between both orifices emerges as a key variable. If the orifices are far

enough, the effect is negligible and the system behaves as if there were two independent silos; otherwise, when the orifices are close to each other, the interaction becomes increasingly important. Besides, it is interesting to note that the intermittent blocking and unblocking of both orifices can provoke the mixing of the granular matter, as reported in (Kamath et al. 2014).

Another variable that is known to strongly affect the clogging probability and is intimately related with the effect of the obstacle described above is the density of particles in the outlet neighborhood. In fact, if the number of particles above the orifice is controlled by modifying the inflow rate of grains into the silo, it can be observed that there is a threshold value above which the grains start to accumulate. Only in this scenario, and if the orifice is small enough, clogging may appear (Hou et al. 2003; Kohring et al. 1995). In this sense, a connection can be made with an experimental work of Roussel et al. where a suspension of grains was made to pass through a mesh with a typical hole size slightly larger than the particle size (Roussel et al. 2007). In particular, it was shown that the proportion of material that was trapped in the mesh (called residual R) strongly depended on the hole size but also on the number of particles per volume unit (solid fraction). Indeed, for outlet sizes as small as two times the particle size (where clogging in a standard silo happens very quickly) it was found that R is negligible for 4% solid fraction samples (Fig. 12). This behavior was reproduced with a model in which the likelihood of clogging was linked to the probability that a given number of particles coincide above an orifice; therefore, higher packing fractions lead to higher probabilities of clogging. The dependence on the outlet size was reproduced by determining that the number of particles necessary to form a clog, n, depended on the hole size as $n = \gamma R^2$. Interestingly, the trend displayed by the residual as a function of R shown in Fig. 12 closely resembles the one reported by To for the probability that a silo with a single orifice jams before emptied (J), as shown in Fig. 4, left. Finally, let us mention that the dependence of the clogging probability on the concentration of particles above the orifice has been also observed in a recent work of Koivisto and Durian, as well as in complementary experiments of fluid driven flow of suspensions through single orifices performed by Wu and coworkers (Guariguata et al. 2012; Lafond et al. 2013).

Regarding the dependence of the clogging probability on the packing fraction above the orifice, Uñac et al. went a step further and revealed the importance of the grain arrangements in the development of clogging inside the silo prior the discharge (Uñac et al. 2012). Their protocol consisted in applying a series of taps of an intensity Γ to a column of grains previous to their discharge through an orifice at the bottom of the

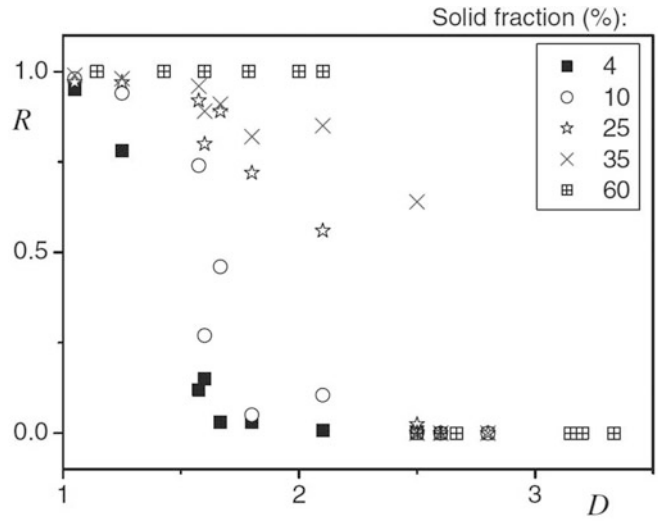

Statistical Mechanics of Clogging, Fig. 12 Proportion of material trapped in the mesh (R) as a function of the mesh hole, in a suspension of particles of different solid fractions as indicated in the legend. (Reprinted from Roussel et al. (2007))

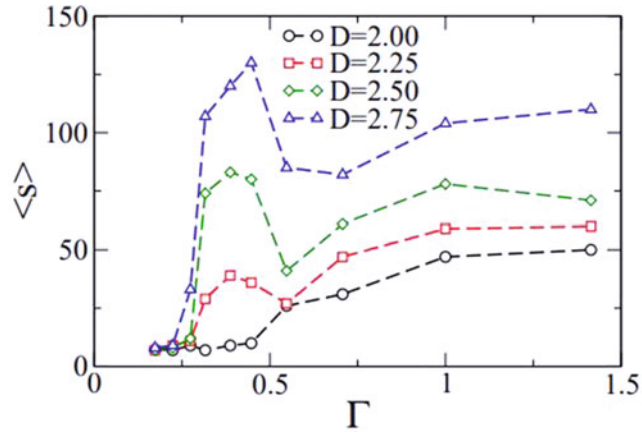

Statistical Mechanics of Clogging, Fig. 13 Mean avalanche size versus the intensity of taps used to prepare the sample before opening the orifice at the bottom. (Reprinted from Uñac et al. (2012))

column. Remarkably, very low values of Γ – which are known to induce very high values of volume fraction – lead to very small avalanche sizes, that is, high probability of clogging (Fig. 13). Nevertheless, the authors also reported that samples with the same volume fraction but generated with a different intensity of tapping gave rise to a different clogging probability. This fact revealed that, in very dense granular matter, the volume fraction is not a good macroscopic parameter for predicting the size of the avalanches that would flow through a given aperture.

Influence of Particles Properties

Apart from the morphology of the exit or the concentration of particles above the orifice, clogging is also affected by the properties of the grains. After a revision of the articles dealing with this issue, it can be concluded that the shape of the grains and the grain to grain friction are the two most influential ones concerning the development of clogging.

It was K. To in his pioneer work (To et al. 2001) who first analyzed the role of friction in the development of clogging from a statistical point of view. He observed that the probability of clogging increased when using toothed disks instead smooth ones (Fig. 14). This phenomenon was linked to the appearance of local convexities in the arches; that is, particles hanging below the line joining the center of their two neighbors. Of course, these configurations are only possible because of friction. Independent confirmation came a few years later when Pournin et al. studied the effect of friction in a systematic way combining experimental and numerical approaches (Pournin et al. 2007). They observed that clogging decreased when reducing the friction coefficient μ; indeed, for the limit case of $\mu = 0$ (analyzed numerically) clogging was dramatically reduced. Clearly, in this unrealistic situation, arches can only adopt regular shapes, and local convexities are forbidden as it was previously illustrated when inspecting the arches developed in a granular column (Pugnaloni et al. 2006).

Experimentally, this issue was confirmed by using frictionless (or almost frictionless) hydrogel particles (Ashour et al. 2017a; Hong et al. 2017). In these works it was reported that even for very narrow bottlenecks (of around 2 or 2.5 times the particle size) the probability of clogging was very small. Interestingly, Hong et al. (2017) demonstrated that using droplets (which are frictionless and deformable at the same time) flow can be attained even for an outlet size equal to the particles. In addition, it was shown (Ashour et al. 2017a) that reducing the friction coefficient prevented the pressure saturation at the bottom of the silo, a phenomenon known as the Janssen effect (Janssen 1895).

As mentioned above, the other outstanding property of grains regarding clogging is the particle shape (Ashour et al. 2017b; Goldberg et al. 2018; Tang and Behringer 2016; Vamsi Krishna Reddy et al. 2018). Tang and Behringer observed that clogging in a 2D silo was enhanced when

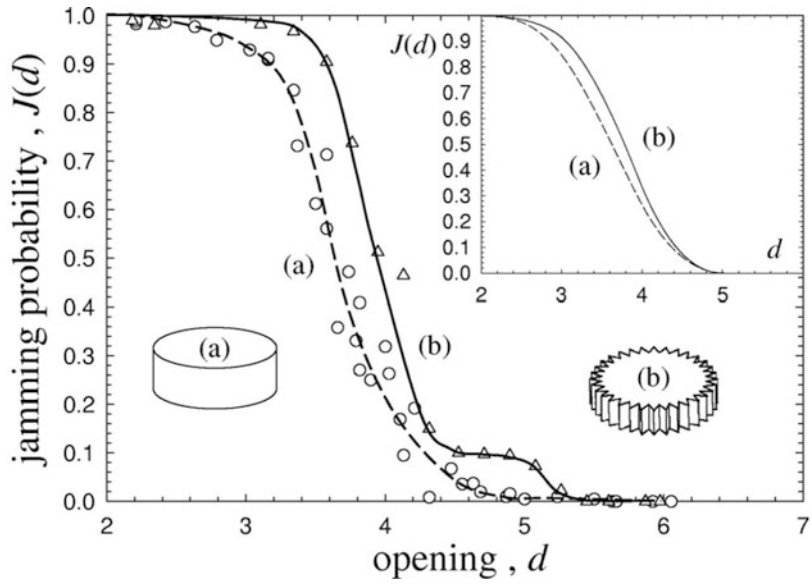

Statistical Mechanics of Clogging, Fig. 14 Probability that a silo gets clogged before all the grains are discharged for smooth disks (a) and toothed disks (b). (Reprinted from To et al. (2001))

using elliptical cylinders because they align with each other, thus increasing the probability of forming stable arches. Also, they suggested that the relevant particle length scale to compare the behavior of ellipses and isotropic grains is the major diameter of the former, and they demonstrated that the number of particles conforming the arch was considerably higher when using anisotropic grains. In a subsequent work, Ashour et al. (Ashour et al. 2017b) confirmed this observation in a 3D silo, and correlated it with the preference of the elongated particles to orient with the longer axis perpendicular to the clogging dome. This orientation was quantified by using X-ray tomography. Again, in this work it was found that an increasing aspect ratio of the grains leads to higher clogging probabilities compared to spherical grains. Notably, for aspect ratios smaller than 6, the mean avalanche size dependence on the outlet size nicely agreed with the divergent fitting expression (Eq. 3) proposed for discs, which was already found to be valid for rice grains (Zuriguel et al. 2005). Nevertheless, a new feature was discovered for particles with aspect ratios larger than 6: whereas for small outlet sizes the mean avalanche size dependence on the outlet size resembles all the other cases, above a given outlet size the experimental data fall below the expected values given by the fitting curves. For even higher aspect rations (above 8) the development of ratholes (completely emptied regions in the central part of the silo surrounded by material close to the lateral wall) strongly alter the clogging dynamics.

Apart from the aspect ratio, another feature of the particle shape that strongly affects clogging is the presence of flat faces (Ahmadi and Hosseininia 2018; Goldberg et al. 2018). By means of discrete element modeling, Goldberg et al. evidenced that polygonal particles clogged more easily than discs. Indeed, the polygons that were more prone to clog a two dimensional silo were shown to be the squares, and then hexagons, pentagons, triangles, and heptagons – which displayed a much smaller probability of clogging (close to that of discs). The reason for this behavior was found to be in the number of side to side contacts among the particles due to shearing forces: squares where the most likely to be aligned and develop this kind of highly stable contact, whereas these configurations were most rare in heptagons. Also, in a recent work in which both gravel and spherical beads were used, more clogging and taller arches were found with gravel (Ahmadi and Hosseininia 2018). Interestingly enough, all the results obtained with these different materials have been accounted for using the peak friction angle, which was found to be the

main parameter controlling the stability and dimension of the clogging arches.

Finally, let us mention that other variables such as the particle size dispersion (Chevoir et al. 2007; Pournin et al. 2007; Zhao et al. 2019) or the particle size (Gella et al. 2018) have been also shown to affect the clogging probability. Regarding polydispersity, Pournin et al. (2007) performed experiments in a 3D silo with both monodisperse and bidisperse samples, evidencing that jamming mainly depends on the volume averaged diameter of the sample. However, care must be taken when the size difference among the particles is large enough to induce segregation; in this case clogging propensity was enhanced. Opposite to these results, in a recent work based on DEM simulations, Zhao et al. (2019) revealed that increasing the polydispersity of the particle sizes in the silo enhances the probability of clogging. To reach this conclusion, they worked with different samples where the particles distributions were lognormal with the same mean particle size but different standard deviation. Then, although the polydispersity role was shown to be less important than the mean particle size, it was discovered to be relevant for some configurations. Interestingly, the same conclusions were attained a decade before when studying clogging of grains through a sieve (Chevoir et al. 2007).

Role of Dynamics on Clogging

Up to now, all the variables that have been related to clogging concern geometrical features, characterizing either the orifice (where the outlet size is the most influential) or the particles (shape, polydispersity, and so on). Also, the effect of other parameters such as the volume fraction above the orifice has been identified as potentially relevant. Nevertheless, the role of kinematics in the development of clogging has not been addressed yet, even though the influence of some geometrical aspects of the silo on clogging has been explained through a connection with this parameter. This is the case of a recent work where the influence of the silo width on the clogging probability was linked to an alteration of the particles movement above the outlet (Gella et al. 2017).

Concerning the role of particle dynamics on clogging, Dorbolo et al. performed pioneer silo discharge experiments in high and low gravity conditions, studying gravity values above and below the Earth's gravity (Dorbolo et al. 2013). Although this work was mainly focused on the flow regime (i.e., when clogging does not happen), it was tentatively reported that gravity did not strongly affect clogging behavior. This result was confirmed afterwards by Arévalo et al. (2014), who performed systematic numerical simulations of clogging in a silo with a fixed outlet size (3.5 times the particle size) varying the gravity values over four orders of magnitude. Despite this huge variation, the avalanche size only changed slightly, increasing 1.6 times when going from 0.001 g to 10 g. In a subsequent work, this result was qualified and it was shown that the effect became more important when increasing the outlet size, as it happened with the obstacle effect. For the largest outlet investigated, the avalanche size increased 10 times for the same variation of 4 orders of magnitude in the gravity value. This discovery was explained by portraying the clog formation as a double step process: first, an arch spanning the outlet size must be formed; and second, the arch must resist until the complete dissipation of the kinetic energy in the system. Indeed, this approach allowed estimating the probability that an arch is destabilized, which was shown to primarily depend on the square root of the system kinetic energy.

Following this idea and aiming to design an experiment that better isolates the contribution of the kinematic effects on the clogging process, Gella et al. built a setup consisting of an extracting belt below the silo orifice. This device allows to control the grain mean velocity without changing the outlet size, effectively decoupling these two variables. Using this strategy, it was revealed that clogging dramatically increases when the grains are discharged at very low velocities (in a quasi-static manner). Moreover, the geometrical and

kinetic contributions to the clogging process in a 2D silo were nicely decoupled and described by an expression (Eq. 5) which was inspired in the stretched exponential proposed by K. To (2005) and D. Durian (Thomas and Durian 2015).

$$P_c = (a + bv)^{-\left(R/d_p\right)^2} \tag{5}$$

Remarkably, this new expression included only two fitting parameters to describe all the results obtained when varying both the outlet size and the velocity of the grains. The first parameter (a) accounts for the geometrical effects of clogging and was the only one affecting the value of the probability of clogging in the quasi-static regime, that is, when the velocity of the grains tends to zero. The second (b) accounted for the kinematic effects and enters Eq. 5 as a factor the velocity of the grains v. As the experiment was performed in 2D, the exponent was the rescaled outlet size raised to the power of 2. The authors demonstrated that this expression (with the same fitting values) was also valid to reproduce the data obtained in a standard silo (discharged purely by gravity without a conveyor belt) if the velocity of the grains is replaced by the well-known relationship $v = \sqrt{gR}$ proposed in Beverloo et al. (1961).

Arches

As clogs are caused by the formation of arches, it is natural to study the properties of these mesoscopic structures and try to establish a relationship between them and the macroscopic behavior. For example, it is interesting to establish a connection between the microscopic properties of the particles conforming the arch, and its shape or stability. We will now approach the topic of the arch shape and its relationship to clogging.

A natural way to describe the arch shape is through the angles subtended between the centers of consecutive beads (Fig. 15): the center of every three beads in contact subtends an angle ϕ, and therefore the set $\{\phi_i\}$ is a straightforward way to define the shape of an arch blocking the exit orifice. In the model of To (see Fig. 4, right) these angles must be smaller than 180° (To et al. 2001). This is a good approximation because most of the beads indeed fulfill this condition, and if friction is very small this should hold. Nevertheless, in experiments it is found that angles can be higher than 180°, meaning that the beads associated to that angle are hanging from the neighbors due to friction. In one particular realization using a flat bottomed hopper it was found that the proportion of such beads was as high as 17% (Garcimartín et al. 2010). They were called defects, and it can be surmised that they will be rather unstable against perturbations. Although in principle this result would contradict To's ideas, it turns out that the model is quite representative of the real behavior. The reason is that successive angles are anticorrelated (Garcimartín et al. 2010), meaning that a big angle is likely to be found before a small one, and vice versa. Therefore if angles are taken in pairs the average is very likely below 180°, as assumed by the model of To. Finally, let us note that particle shape and friction are paramount in determining how large the angles can be. As reported in To's article of 2001 enhanced friction, as achieved with dented disks, largely increased clogging probability. In particles with flat faces, this effect is exacerbated (Ahmadi and Hosseininia 2018; Goldberg et al. 2018).

If a hopper is considered instead of a flat-bottomed silo, then the hopper angle introduces a boundary constraint that determines the maximum values of the angles θ between the segment joining the centers of two consecutive particles and the horizontal (see Fig. 16e). López and coworkers (2019) proposed that for hypothetically frictionless particles in a hopper having an angle β with respect to the horizontal, the angle θ_1 formed by the first two particles (starting from the left) would necessarily be smaller or equal to $(90° - \beta)$. Otherwise, the first particle would be unstable. Then, following To's idea (To et al. 2001), the second angle θ_2 should be equal or smaller than θ_1, and so forth, until the last one

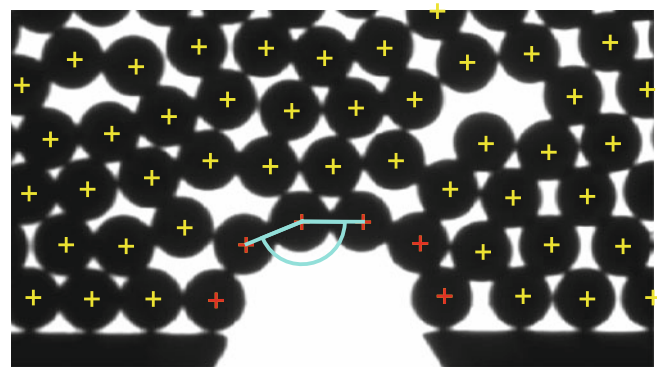

Statistical Mechanics of Clogging, Fig. 15 Photograph of a clogging arch in a flat bottomed 2D silo. The angle formed by the centers of three beads is defined as ϕ. (Reprinted from Lozano et al. (2012b))

θ_{n-1}, which must fulfill the condition of being larger than $-(90^\circ - \beta)$. Therefore, all the angles 9 should fall within a range determined by the hopper angle as denoted by the following equation:

$$\left(90^\circ - \beta\right) \geq \theta_1 \geq \theta_2 \geq \ldots \geq \theta_{n-1} \geq \left(90^\circ - \beta\right) \tag{6}$$

Experimental results are in good agreement with this interpretation (see Fig. 16), although some values of θ are also observed beyond these limits, a behavior that was attributed to friction.

As a consequence of the restriction of possible angles provoked by the hopper walls, it happens that the number of allowed arches is drastically reduced as the hopper angle increases. Consequently, the clogging probability diminishes. Besides, for large hopper angles, the narrow range of angles allowed (see Fig. 16d) imposes that arches are almost flat; as a consequence, the number of beads in the arch becomes discretized and the clogging probability changes stepwise with the size of the exit orifice. This contrasts with the case of a flat bottomed silo, where the distributions are rather wide (see Fig. 16a). In this case, it was shown that the arches display a wide variety of shapes, although they tend to be semicircular when the outlet size was enlarged (Garcimartín et al. 2010).

An interesting question in relation with the arch shape concerns their connection with the forces that they withstand. This relationship can only be statistical: it is impossible to establish a univocal correspondence between shape and force, as one arch shape can tally with many different force distributions. In two dimensions, Valdes and Santamarina (2008) pointed out that the mean force orientation in the packing would determine the optimal arch shape: for vertical and horizontal average forces, the optimal shape is parabolic or a catenary; and for a uniform force orientation distribution, the optimal shape is semicircular. In fact, the semicircular shape observed for large arches in Garcimartín et al. (2010) was attributed to a uniform orientation of the forces within the silo. Although arches are not necessarily an optimal response to the orientation distribution of forces, this result can be taken as a hint, showing how shape can provide valuable information about the forces.

Unfortunately, the measurement of the forces at the grain level is not easy (Daniels et al. 2017) and, as far as we know, it has been never systematically performed for clogging arches. Therefore, all the knowledge we have about this topic comes from numerical simulations, as in the work of Pugnaloni and collaborators (2006) where the forces in the arches developed within a column of grains were analyzed. Forces in clogging arches have been investigated in Hidalgo et al. (2013) and Longjas et al. (2009). Indeed, in Longjas et al. (2009) the forces were used to infer the proportion of possible arches that would be stable and, therefore, able to cause clogging. However, this analysis was limited to arches of three particles. In a

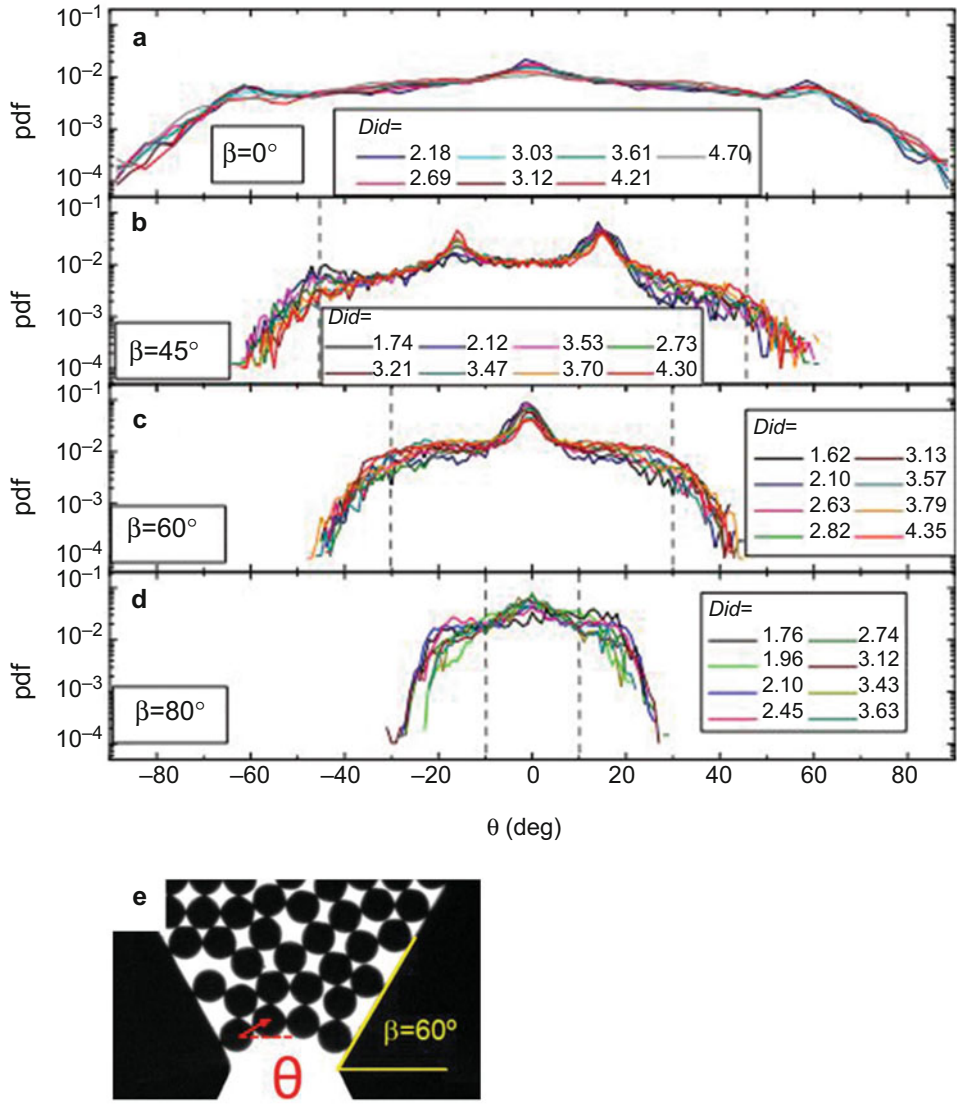

Statistical Mechanics of Clogging, Fig. 16 (**a**–**d**) Probability distribution function of the angle θ between the centers of two consecutive particles in an arch and the horizontal, as indicated in (e). β is the angle that the hopper makes with the horizontal. In a–d the curves represent values of θ obtained for different outlet sizes (as indicated in the legend), and the vertical dashed lines, the limit values that would be imposed by the hopper walls for a frictionless sample. (Reprinted from López-Rodríguez et al. (2019))

subsequent work (Hidalgo et al. 2013), molecular dynamics simulations were used to unveil that the normal forces within the particles conforming the arch are, in average, much larger than the ones among particles in the bulk. In addition, an important relation among the angle subtended among every three particles ϕ and the average force was observed: the larger the angle, the higher the tangential, and the lower the normal force. Therefore, the higher the angle, the higher the friction mobilized to sustain the particle. This result is consistent with experimental data reported in the following chapter concerning the resistance of arches against perturbations.

Unclogging

Once an arch that blocks the orifice is formed, in principle it will last forever. The formation of an arch involves a mechanically stable configuration, and therefore a perturbation is needed to break it. This may come in different forms. Thermal cycles, for instance, may make the grains dilate and contract, hereby disturbing the contact forces. Although this method has not been used specifically to unclog a silo, it was shown that this procedure can compact a granular medium, which is closely related to breaking arches inside it (Divoux et al. 2008). Local perturbations on the grains at the orifice, for instance with a fluid jet (Zuriguel et al. 2005), or a movable orifice (either oscillating (To and Tai 2017) or rotating (To et al. 2019)) have also been used. However, an external vibration is probably the most extended method to restore flow when an orifice clogs; this is especially true in industry and applications, where silos and hoppers with the addition of a vibrating mechanism are often used. Indeed, vibrations can be also coupled to air injection to fluidize granular materials stored in industrial silos, especially of cohesive grains (Wes et al. 1990). Finally, the vibration of lateral walls as a means of enhancing the flow has been also proved to be a good alternative (Pacheco-Martinez et al. 2008).

Among all these ways to disturb the clogging arches and resume the flow, we will focus here on vertical vibrations applied to the silo bottom or to the whole silo. The reason is that this situation allows for a relatively easy way to quantify the strength of the external perturbation introduced. As a matter of fact, a silo submitted to a sinusoidal vibration of frequency f and amplitude A is relatively easy to implement in the laboratory. Importantly, it has been shown (Wassgren et al. 2002) that the flow rate of a vibrated silo does not change drastically with respect to a static one, provided that the amplitude is small and the frequency is higher than the characteristic time of the dynamics (Chen et al. 2006; Evesque and Meftah 1993; Mankoc et al. 2009; Suzuki et al. 1968). This allows a straightforward comparison of vibrated and static silos. Indeed, in a vibrated silo with a small orifice it was shown an intermittent flow in which the distribution of flow intervals follows an exponential distribution (Mankoc et al. 2009). As explained in chapter Clogging as a Stochastic Process for the avalanche size distribution, this means that the probability of clogging is constant along time, and that clogging events are uncorrelated. Therefore a single characteristic time can describe this process, which can be related to the mean flowing time, the clogging probability of a single bead as it passes through the orifice, and the avalanche size. On the contrary, the distribution of clogging intervals revealed wider tails. Notably, the same scenario was found for horizontal vibrations of the orifice (To and Tai 2017).

The nature and specific properties of these tails were studied more closely by Janda et al. (2009b). Although the research was aimed to obtain a delivery device that could release a small quantity of grains in a controlled fashion (and thus some of the experiment details, such as the orifice shape and the vibration mechanism, were highly specific), similar features to the results reported in Mankoc et al. (2009) were observed concerning the dynamics of clogging and unclogging. Again, the flowing intervals were shown to be distributed exponentially, while the duration of clogs was suggested to follow a power law: $\mathrm{pdf}(T_J) \propto T_J^{-\alpha}$ (Fig. 17). This implies the absence of a characteristic time scale for the clog duration, and then, it follows that the probability that a clogging arch is shattered is not constant along time. Remarkably, it was found that for some specific values of the variables, the exponent α of the power law was lower than 2, implying that the average clog duration (calculated with an integral including the probability density function) does not converge. All these facts hint that the process of breaking arches with vibrations involves complex dynamics.

In order to explore how the clogging arches are broken, two broad kind of procedures can be used concerning the kind of vibration applied: either a vibration of growing amplitude (a ramp), or a constant amplitude vibration. In the first case, the intensity of the perturbation grows along time, which is a natural way to probe the force, or acceleration, that arches can withstand. On the

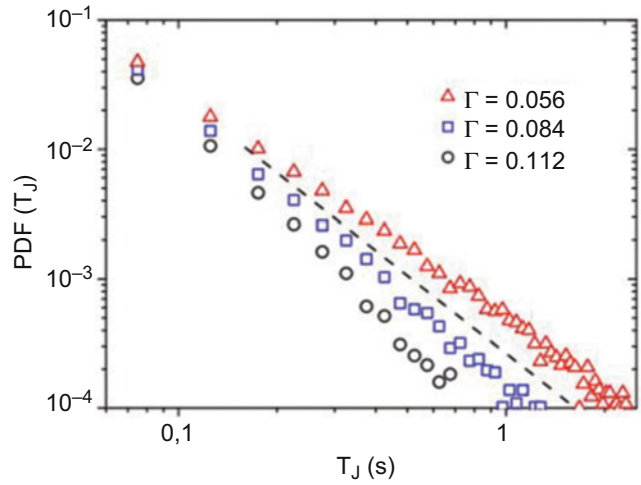

Statistical Mechanics of Clogging, Fig. 17 Log-log plot of the pdf of the time lapses during which the flow is arrested using an inclined hopper with an aperture of around $R = 1.78$ times the particle size. The dashed line has a slope of two so the slope of the distribution for lowest acceleration Γ (see legend) is smaller than this value. (Reprinted from Janda et al. (2009b))

second case, the time that arches last under an imposed perturbation is studied. The next two sections are devoted to explain the investigations related to these different approaches.

The Weakest Link

In order to test the endurance of arches, the idea is to place a silo on top of a shaker and, when an arch is formed, to start a vibration ramp at a constant frequency and a linearly growing amplitude (Lozano et al. 2012b, 2015). Then, the instant when the arch is broken can be measured, and hence the acceleration needed to break it. In addition, if the silo is two-dimensional, the shape of the arch above the orifice can be monitored. As the variable considered here is the force needed to break the arch, the adimensional parameter $\Gamma = \frac{A\omega^2}{g}$ is used to quantify the vibration, which is the maximum acceleration in gravity units (ω is the angular frequency).

The first remarkable result obtained with this protocol is that the shape of the arch is closely related to the acceleration needed to break it (Lozano et al. 2012b). In particular, if we focus on the angles subtended between the centers of adjacent beads (ϕ), then arches having beads with an associated angle larger than 180° (or, *defects*) are the weakest. Indeed, it was found that the larger the maximum angle in an arch ($\phi_{\max}$), the lower the acceleration needed to break it (Fig. 18). Although this is only true in a statistical sense, a linear fit between Γ and $\phi_{\max}$ was proposed for $\phi_{\max} > 180°$: $\Gamma = -C_1(\phi - 80°) + C_2$, where C_1 and C_2 are positive constants that depend on the friction coefficient. This relationship holds for materials with different friction coefficients. By extrapolating the curve, a limit value of $\phi_{\max}$ close to 200° was found for steel beads (the exact value depends on the material). Interestingly, the distribution of ϕ revealed an abrupt decrease at an angle around 200°. Therefore, this figure was interpreted as a cut-off value above which particles cannot be sustained by frictional forces anymore. A simple model was proposed to account for the relationship between Γ and $\phi_{\max}$ explained above.

As a general result, it was concluded that the bead with $\phi_{\max}$ was the weakest link in the arch, especially if that angle was bigger than 180°. Apart from the dependence of the arch robustness on $\phi_{\max}$ explained above, it was also evidenced that the likelihood of the arch breaking precisely at that defect was bigger than in other positions. Then, in a subsequent work (Lozano et al. 2015) these findings were generalized to other acceleration ramps, and several outlet sizes. In particular, it was found that even comparing sets of arches with the same maximum angle, the ones corresponding to larger outlet sizes displayed lower values of Γ, indicating that $\phi_{\max}$ is not the only variable determining the stability of the clogging arch.

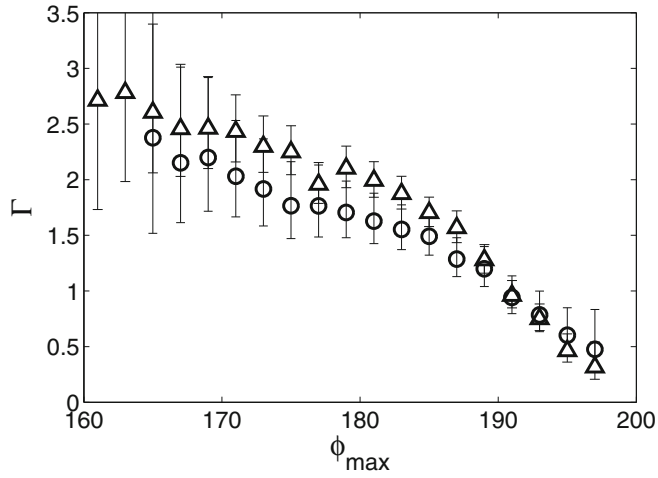

Statistical Mechanics of Clogging, Fig. 18 The average maximum acceleration Γ at the instant of arch breaking, as a function of ϕ_{max}, the maximum angle in the arch. Triangles and circles correspond to steel and brass beads respectively. Error bars are 95% confidence intervals. (Reprinted from Lozano et al. (2012b))

Arch Breaking Is a History Dependent Process

An alternative approach to study the arch breaking process is to apply a constant vibration and measure the breaking time (or, the time it takes for the vibration to shatter the arch and restore the flow). This is analogous to the procedure explained at the beginning of this chapter as implemented in (Janda et al. 2009b; Mankoc et al. 2009). However, in the cases that will be described below, the external excitation was not acting all the time but was started after the formation of a clogging arch that was formed without vibration. With this procedure, it is guaranteed that the arches formed are not broken by the impacts of particles coming from above, or in other words, by the intrinsic noise within the silo before all the kinetic energy is dissipated.

Results of such an experiment were reported in (Zuriguel et al. 2014) where risk analysis was used to describe the time that arches can resist a constant vibration. Let us call t_b the time it takes to break an arch. Then, the survival function S at time t is defined as the probability that an arch lasts more than t. Mathematically,

$$S(t) \equiv P(t_b > t) = \int_t^\infty P(t')dt' \qquad (7)$$

where $P(t)$ is the probability distribution function, or pdf, of t_b. Note that if $P(t) \sim t^{-\alpha}$, then $S(t) \sim t^{-\alpha+1}$. Observations are robust in finding heavy tails (see Fig. 19), meaning that for times larger than a given value ($t_{threshold}$) S decays as a power law. As stated before, this indicates that the probability of breaking an arch is not constant along time. Moreover, it was confirmed that in some cases the exponent α is such that the integral does not converge. In particular, the role of three parameters on the distribution of breaking times was explored in Zuriguel et al. (2014). It was shown that increasing the outlet size or the intensity of vibration leads to a bigger α, whereas an increase of the number of grains above the clogging arch implied a reduction of the exponent. It was also demonstrated that distributions for which the average diverges ($\alpha \leq 2$) took place for low vibration intensities, small orifices, and large heights of the column of grains above the clogging arch (Fig. 19).

In addition, the distributions of Fig. 19 reveal that in some cases the curves flatten for very large times (typically above 100 s). Overall, the trends displayed by the survival functions hint to the following interpretation. When a constant vibration is imposed, some arches break down in a relatively short time (say, a few tenths of seconds). After this time ($t_{threshold}$), surviving arches are harder and harder to break, so the breaking time for these arches lacks any characteristic scale. In this temporal range $S(t)$ is compatible with a power law decay. Finally, it seems that there are a few arches that are even more enduring, so the vibration seems unable to break them, and cause a

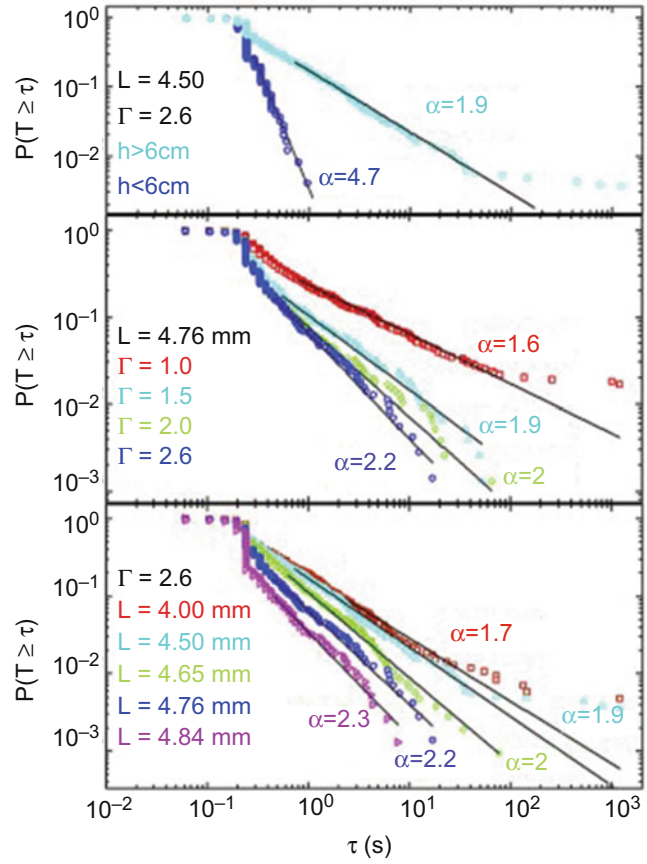

Statistical Mechanics of Clogging, Fig. 19 Clogging time distributions in a two-dimensional silo. (Top) Time lapse complementary CDFs obtained using $L = 4.50$ and $\Gamma = 0.26$ for two different heads of grains above the silo bottom ($h < 6$ cm and $h > 6$ cm). (Middle) Time lapse complementary CDFs obtained for $h > 6$ cm, $L = 4.76$ and several Γ as indicated in the legend. (Bottom) Time lapse complementary CDFs obtained for $h > 6$ cm, $\Gamma = 0.26$, and several outlet sizes as indicated in the legend. (Reprinted from Zuriguel et al. (2014))

final flattening of the distribution. This latter result was confirmed in Lozano et al. (2015) where for some of experimental conditions the distribution almost completely flattened after a time of about 50 to 100 s, suggesting that there are some arches that the vibration cannot break for the parameter range explored.

In order to unveil the origin of the broad tails of the breaking times distributions and the final flattening, Guerrero et al. analyzed the movements of individual beads in an arch along time prior to their collapse (Guerrero et al. 2018). They observed that under a gentle, constant vibration, the beads hardly move except for fast rearrangements (fast meaning that they take place in a short time compared to the life of the arch). This can be observed by plotting the temporal evolution of the values of $\{\phi_i\}$ for all the beads in the arch. Alternatively, one can use a single number: σ (the standard deviation of all the values ϕ_i found in a given arch) which captures the rearrangements of the arch as illustrated in Fig. 20.

A key feature that can be deduced from these time series is that the angle rate of change is not proportional to the angle itself. From experiments with a vibration ramp one could have naively expected that at least the bead associated to the biggest angle (the most dangerous one) would evolve in such a way that its angle would monotonously grow until it reached the point of collapse. This is not the case if the arch is submitted to a gentle, constant vibration. The evolution of individual angles is much more complex than that.

In order to analyze the slow relaxation dynamics, one can calculate the two time autocorrelation function of σ, for a lag time τ and a waiting time t_w:

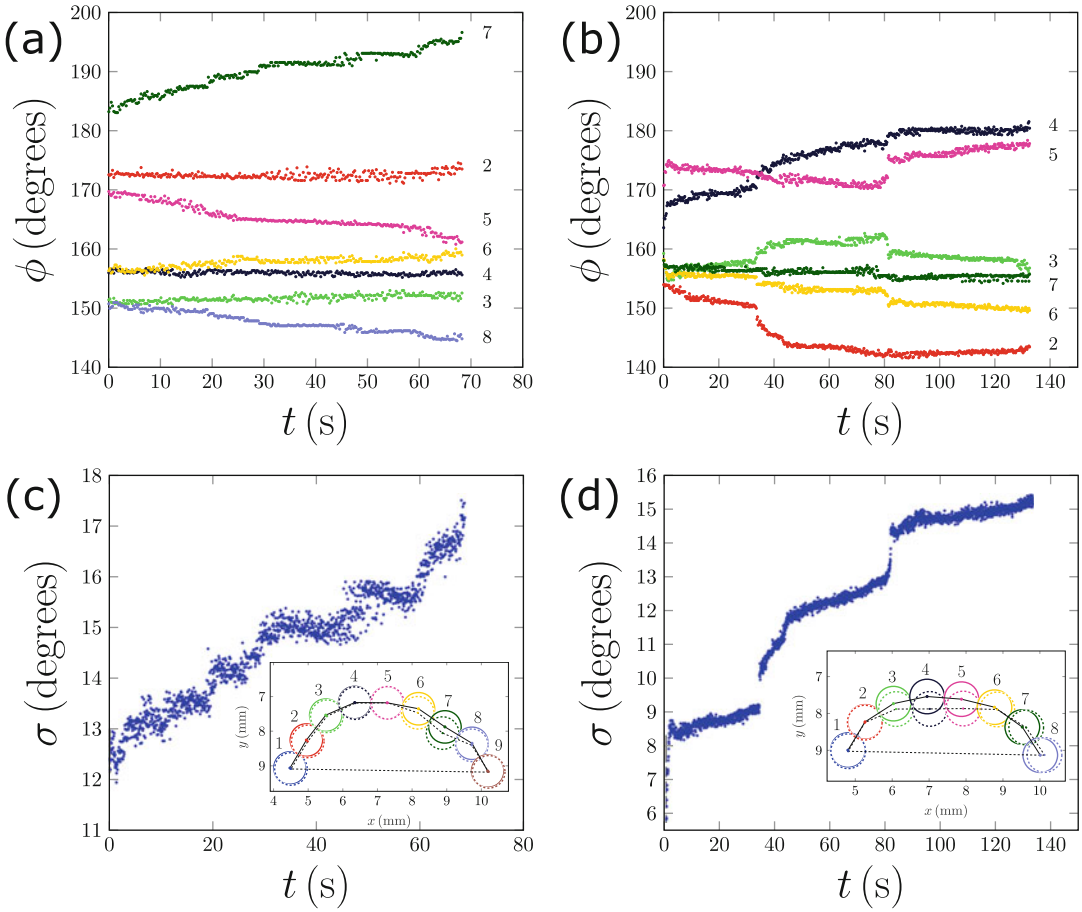

Statistical Mechanics of Clogging, Fig. 20 Evolution of two different long-lasting broken arches, (a) plus (c), and (b) plus (d). Upper panels show $\phi(t)$ for each grain. The lower panels show σ (the standard deviation of all the values ϕ_i found in a given arch). The color and the number on the right side of each $\phi(t)$ curve indicate the bead of the arch (see the insets in lower figures). The inset shows the position of each bead of the arch at two instants: just after starting the vibration (solid line) and just before the collapse (dashed line). Reprinted from Guerrero et al. (2018)

$$C(t_w, \tau) = \frac{\langle \sigma(t_w + \tau)\sigma(t_w)\rangle - \langle \sigma(t_w + \tau)\rangle\langle \sigma(t_w)\rangle}{\sqrt{VAR(\sigma(t_w))VAR(\sigma(t_w + \tau))}} \tag{8}$$

where $\langle \ldots \rangle$ denotes the ensemble average. It was found that the correlation decreases with τ; but notably, it also depends on t_w, denoting that the process is not stationary along time. For long waiting times, C tends to a limit value. It had been pointed out (Nicodemi and Coniglio 1999) that aging effects often show a logarithmic dependence on this time, and this was precisely the behavior observed for the dependence of C on t_w for a fixed τ.

Aging is a nonergodic process in which the ensemble average and the time average are not equivalent. Some models have been proposed to explain the behavior of these arches. Nicolas and coworkers (2018) considered that the arch being vibrated is able to explore an energy landscape in which traps represent more stable configurations. Using a simple shape for the energy wells and the escape rate proposed by H. Kramers (1940), a survival function that reproduces the basic features of the experimental observations was obtained. Also, in an effort to understand nonergodicity, C. Merrigan and coworkers (2018) rationalized the intermittent motion of the beads as a continuous

time random walk of a vector whose components are the angles $\{\phi_i\}$ of the arch. They simulated vibrated arches and noted how this model is consistent with ergodicity breaking. They went on to compare some of the numerical results with experiments, finding an overall good agreement, notwithstanding several discrepancies (Guerrero et al. 2019). The notion of the arch performing a random walk in the space of locally stable arch shapes, where each shape is characterized by a dwelling time that depends on the depth of the trap, is therefore quite reasonable.

Summary and Discussion

Along this work we have summarized the existing knowledge about clogging of macroscopic inert particles when passing through a constriction. The typical instance of this scenario is the discharge of a silo through a small orifice, a system in which it is well accepted that the development of clogging can be described as a Poisson process. The reason behind this is that the emergence of a clog is equally likely at any time during the discharge. In practice, this feature is typically inferred from the statistics of the avalanche sizes which, in all cases but in narrow slits, reveal an exponential tail. This implies that the mean avalanche size (as well as the mean avalanche duration or the probability of clogging) is always well defined.

As a matter of fact, for its simplicity and easiness to obtain, the avalanche size is often used to characterize the effect of different variables on clogging development. Among these variables, the most influential is clearly the outlet size (or more precisely, the ratio between the outlet and particles size). Indeed, it is known that the mean avalanche size abruptly grows when this parameter is increased. The question about the existence of a critical outlet size above which clogging is not possible is still open, although mounting evidences suggest that the clogging transition is similar to the glass and jamming ones. In these cases, relaxation times grow dramatically but do not necessarily imply the existence of a critical point.

Concerning other parameters that affect clogging, we have underlined the role of two: the volume fraction and the velocity of the grains at (or near) the orifice. The former is a contributing factor, as it determines the probability that a given number of grains coincide above the outlet and form an arch. The latter, however, has been argued to affect the number of these arches that are able to become stabilized and survive after all the kinetic energy within the system is dissipated. Then, the higher the velocity of the grains, the smaller the number of arches that are stable, and therefore the lower the probability of clogging. Interestingly, the reason for which a suitably placed obstacle above the orifice is able to dramatically reduce the clogging probability can be associated to an alteration of these two parameters: the obstacle reduces the pressure, confinement and packing fraction near the orifice (so it prevents arch formation), and besides, it alters the velocity field increasing the kinetic energy of the grains at the outlet (so it prevents arch stabilization).

Once a clog is formed, an external input of energy is necessary to resume the flow. The most widely employed method to perform this task is to apply a vibration (either locally at the exit, or to the whole silo). For low intensity vibrations, it has been reported that the distributions of breaking times (i.e., the time that takes since the vibration is applied until the collapse of the arch) display fat tails. These tails can be fitted to power laws, whose exponents depend on different parameters such as the intensity of vibration, the outlet size, and the height of the layer of grains within the silo. It has been remarked that in some cases, the exponent of the power law is smaller than two, a feature implying that the first moment of the distribution cannot be calculated as the integration does not converge.

It is noteworthy that the different nature of the flowing and the clogging times – the former being an exponential distribution, and the latter displaying a power law tail – has also been observed in the passage through bottlenecks of other discrete systems. In particular, it was experimentally shown (Zuriguel et al. 2014) that the flow of sheep through narrow doors displayed an intermittency that could be described within this

framework. Moreover, in this scenario, the distribution of clogging times when placing an obstacle in front of the door revealed an exponent higher than obtained in a standard entrance (without obstacle); this implies a beneficial effect of the obstacle as it reduces the number of long lasting clogs. In the same work, simplistic simulations of pedestrian evacuations through a bottleneck also showed how reducing the desired speed of the agents (which in a congested scenario amounts to diminishing the driving force) lead to an augment of the power law exponent, improving the flow. The same effect was reached when increasing the outlet size or the intrinsic noise included in the movement of these bodies. Finally, in a simulated colloidal suspension, it was also observed an augment of the exponent when increasing the bath temperature.

Considering all these outcomes, a phase diagram of sorts was proposed to account for the clogging behavior in different systems of solid particles flowing through bottle-necks (Zuriguel et al. 2014). The order parameter introduced was $\Phi = \frac{\langle t_f \rangle}{\langle t_c \rangle + \langle t_f \rangle}$ where $\langle t_f \rangle$ is the average duration of the flow intervals and $\langle t_c \rangle$ is the average clog duration. As $\langle t_c \rangle$ only converges when the exponent α of the power law is larger than two, $\alpha \leq 2$ implies $\Phi = 0$; a feature that was proposed to qualify the "clogged state." On the contrary, when $\Phi > 0$ it can be said the system is in an "unclogged state." In the latter scenario, the flow can be either continuous if $\Phi = 1$, or intermittent if $0 < \Phi < 1$. From this, the effect of the different variables in the values of Φ was tested, checking that the system could reach the clogged state (i.e., $\Phi = 0$) by decreasing the exit size and reducing the particle's excitation (intrinsic or external). Also, augmenting the pressure at the narrowing seemed to drive the system to a clogged state. According to these findings, and inspired along the concepts of compatible and incompatible load introduced by Cates et al. at the end of the last century (Cates et al. 1998), all the variables affecting clogging were encompassed in three general magnitudes: the characteristic size of the neck (λ), the incompatible load (I_L) and the compatible load (C_L) as depicted in Fig. 21 (left). For the case of a vibrated silo, a more detailed phase diagram for the plane $\Gamma - D$ (which in the framework of the generic variables corresponds to the plane $I_L - \lambda$) was reported in Zuriguel et al. (2017) (see Fig. 21, right).

In recent years, several lines of investigation have reported a number of results which are congruent with the proposed global framework. For example, real pedestrian drills evidenced that the stronger the force applied by the crowd in their way out of a room, the slower the evacuation (which can be considered as a slightly modified version of the traditional Faster is Slower phenomenon in pedestrian dynamics) (Pastor et al. 2015). The reason behind this behavior was on the increment of the clogging times with a higher force (compatible load). Also, it seems that the increment of the compatible load was behind the transition from unclogged to clogged states reported for the flow of small robots (Vibration-Driven Vehicles) when passing through a narrowing (Patterson et al. 2017). In that case, instead of altering the force of each individual, the increment of the compatible load was achieved by increasing the number of agents inside the room.

Apart from the interest of the phase diagram from the point of view of clogging, its resemblance to the scheme introduced for the jamming transition by Liu and Nagel (1998) has stimulated recent investigations on the relation among these two states. In principle, clogging and jamming are two well-differentiated phenomena: clogging is a local occurrence triggered by the formation of a mesoscopic structure (an arch) that is able to arrest the grains (or bodies) behind it; on the contrary, jamming is a global state of the matter where different kind of spatially averaged quantities can be measured and used to characterize the system response.

Recently, Reichhardt and collaborators have started to investigate the connection between these two phenomena (Nguyen et al. 2017; Péter et al. 2018). To this end, they have developed numerical simulations of the flow of particles through arrays of obstacles, implemented as pinned particles (see Fig. 22, left). Then, depending on the number of pinned and mobile particles, the system was found to reach different

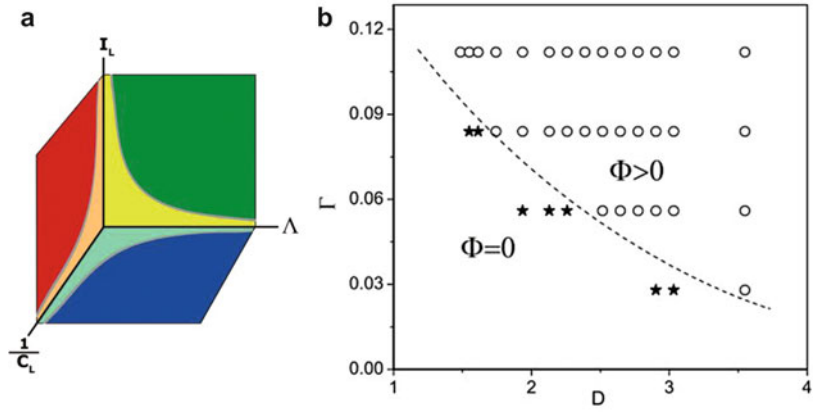

Statistical Mechanics of Clogging, Fig. 21 Left, generic phase diagram proposed for the flow of many-particle systems through bottlenecks. Right, phase diagram for the plane $\Gamma - D$ obtained for the locally vibrated eccentrically discharged hopper used in (Janda et al. 2009b). Stars indicate points where $\Phi = 0$ (clogged phase) and circles show positions where $\Phi > 0$ (unclogged phase). The dashed line is a guide to the eye suggesting a possible boundary between the two phases. (Reprinted from (Zuriguel et al. 2014) (left) and (Zuriguel et al. 2017) (right))

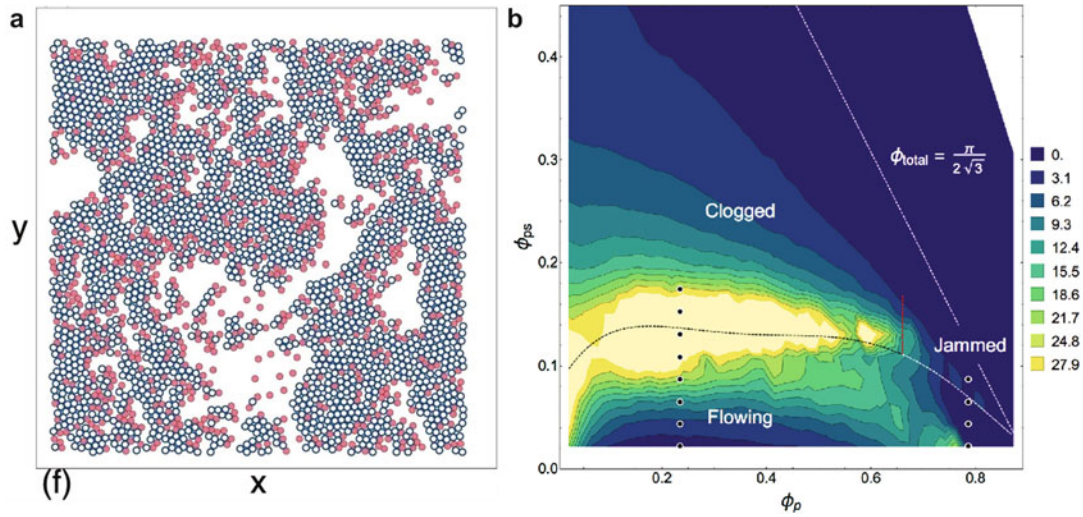

Statistical Mechanics of Clogging, Fig. 22 Left: Final clogged state of mobile disks (blue open circles) driven in the positive x direction through obstacles (red filled circles) in a sample with obstacle density $\phi_{obs} = 0.175$ and disk density $\phi_m = 0.436$. Right: Map of the transient times τ obtained depending on ϕ_{obs} vs ϕ_m. Yellow corresponds to large τ and blue to small τ as indicated in the legend. The dark dashed line is a guide to the eye marking the crossover from a flowing state to a clogged state, while the white dashed line indicates the transition from a flowing state to a jammed state. In the white region, there are not data as it is above the maximum density that could be reached in the implemented model. (Reprinted from Péter et al. (2018))

stationary states: fluid, clogged, or jammed, as illustrated in Fig. 22 (right). Remarkably, the clogging transition was reported to have characteristics of an absorbing phase transition in which, after a transient time, the system evolves into a heterogeneous state as the one represented in Fig. 22 (left). This transient time was shown to diverge at the transition as illustrated by the yellow region in Fig. 22 (right). In contrast, jamming was proved to be a rapid process in which the

sample does not reveal any sign of heterogeneity. In this case, the magnitude that diverges as the jamming density is approached turns out to be the rigidity.

All these results – which are similar to the ones reported in a previous work of Tejada et al. (2016) – have been partially confirmed by Stoop and Tierno in experiments where they drove colloidal monolayers across different arrays of obstacles (Stoop and Tierno 2018). Remarkably, in the experimental conditions implemented in this research, the Faster is Slower effect –characteristic of the flow through bottlenecks of pedestrians – was also identified. Again, this is another evidence that supports the existing connections on the behavior of different many-body systems when flowing through constrictions.

Future Directions

Although the amount of knowledge gained in the last two decades on the silo clogging problem is rather considerable, it is also true that the number of questions that are still unanswered is also numerous. Here, we are going to indicate some of the problems we consider more stimulating, either from a fundamental or by an applied point of view.

First, it will be interesting to deepen in the relationship among clogging and jamming. As mentioned above, this topic has been approached within the framework of a simulation where a dense sample of mobile particles flows through a series of obstacles. Although the findings of these simulations have been somehow validated by experiments with colloidal suspensions, it would be nice to see if the same behavior can be experimentally tested using dry macroscopic grains. Also, there are some other systems which may help to shed light on this jamming-clogging connection. One of these is the flow of inert grains through very narrow pipes. In this geometrical configuration, it has been recently shown that clogging is also possible due to the development of hanging arches supported by frictional forces against the wall (Janda et al. 2015; Verbücheln et al. 2015). As in this pipe flow there is not a bottleneck that introduces a local inhomogeneity, it is possible that the conditions leading to clogging are comparable to the ones leading to jamming. In addition, the study of clogging in narrow vertical pipes is of great applied interest as the formation of hang-ups is one of the major problems in ore transportation in underground mining (Hadjigeorgiou and Stacey 2013).

Another issue that should be carefully investigated in the forthcoming years is the parallels among clogging in 2D and 3D scenarios. Although most of the features observed in relation with clogging are similar in two and three dimensions, some differences exist. The most salient one concerns the divergence of the mean avalanche size with the outlet size, which seems to take place in 3D silos but has been practically discarded in 2D ones. In addition, the statistical analysis of the properties of arches and the effect of different variables (such as the hopper angle) has been mostly approached using 2D silos, so an extension to 3D scenarios is needed. This could be tackled by studying the role played by the silo thickness in quasi-two-dimensional geometries, gradually changing from a 2D silo formed by a monolayer of grains to a fully 3D case.

Considering the role of all the different variables summarized in this work, it seems that investigating the effect of combining more than one of these parameters can be fruitful to better understand the physical mechanism behind clogging. For example, knowing the dramatic augment of the probability of clogging occurring when the grains flow through the outlet in a quasi-static manner, it would be interesting to see if in this regime the effect of geometrical aspects (such as the hopper angle or the placement of an obstacle) is similar to the one observed in conditions of free discharge. In this way we will be able to ascertain if the role of these variables is due to its effect on the geometrical or dynamical aspects. Also, further investigation in the configuration where the grains are extracted by an external device (a belt or an endless screw) is important because this is a common procedure in industry.

Doubtless, more investigations are needed in other systems that could also display clogging, such as active matter or pedestrian dynamics. Of

course, this research is not straightforward given the complex nature of the agents involved in these fields and the intrinsic difficulty associated to performing experiments at the micro scale or with pedestrians. Nevertheless, other systems such as macroscopic active materials (or small robots) can be reasonable models in which to incorporate some intrinsic activity to the particles and compare with the behavior of inert granular media. Similar reasoning holds for very promising studies of submerged grains (Koivisto and Durian 2017) and suspended particles (Guariguata et al. 2012; Lafond et al. 2013; Marin et al. 2018), which can be seen as examples with a behavior that is halfway between granular materials and colloidal suspensions.

Bibliography

Ahmadi A, Hosseininia ES (2018) An experimental investigation on stable arch formation in cohesionless granular materials using developed trapdoor test. Powder Technol 330:137–146

Arévalo R, Zuriguel I, Maza D, Garcimartín A (2014) Role of driving force on the clogging of inert particles in a bottleneck. Phys Rev E 89:042205

Arnold P, McLean A (1976) An analytical solution for the stress function at the wall of a converging channel. Powder Technol 13(2):255–260

Ashour A, Trittel T, Börzsönyi T, Stannarius R (2017a) Silo outflow of soft frictionless spheres. Phys Rev Fluids 2(12):123302

Ashour A, Wegner S, Trittel T, Börzsönyi T, Stannarius R (2017b) Outflow and clogging of shape-anisotropic grains in hoppers with small apertures. Soft Matter 13(2):402–414

Beverloo W, Leniger H, van de Velde J (1961) The flow of granular solids through orifices. Chem Eng Sci 15(3):260–269

Cates ME, Wittmer JP, Bouchaud J-P, Claudin P (1998) Jamming, force chains, and fragile matter. Phys Rev Lett 81:1841–1844

Chen K, Stone MB, Barry R, Lohr M, McConville W, Klein K, Sheu B, Morss A, Scheidemantel T, Schiffer P (2006) Flux through a hole from a shaken granular medium. Phys Rev E 74(1):011306

Chevoir F, Gaulard F, Roussel N (2007) Flow and jamming of granular mixtures through obstacles. Europhys Lett (EPL) 79(1):14001

Clément E, Reydellet G, Rioual F, Parise B, Fanguet V, Lanuza J, Kolb E (2000) Jamming patterns and blockade statistics in model granular flows. In: Helbing D, Herrmann HJ, Schreckenberg M, Wolf DE (eds) Traffic and granular flow '99. Springer Berlin Heidelberg, Berlin/Heidelberg, pp 457–468

Daniels KE, Kollmer JE, Puckett JG (2017) Photoelastic force measurements in granular materials. Rev Sci Instrum 88(5):051808

Davies C, Desai M (2008) Blockage in vertical slots: experimental measurement of minimum slot width for a variety of granular materials. Powder Technol 183(3):436–440. Festschrift issue in honor of Professor Robert Pfeffer – articles presented at the honoring session of the AIChE annual meeting in 2006

Divoux T, Gayvallet H, Géminard J-C (2008) Creep motion of a granular pile induced by thermal cycling. Phys Rev Lett 101:148303

Dorbolo S, Maquet L, Brandenbourger M, Ludewig F, Lumay G, Caps H, Vandewalle N, Rondia S, Mélard M, van Loon J, Dowson A, Vincent-Bonnieu S (2013) Influence of the gravity on the discharge of a silo. Granul Matter 15(3):263–273

Drescher A, Waters A, Rhoades C (1995) Arching in hoppers: II. Arching theories and critical outlet size. Powder Technol 84(2):177–183

Endo K, Reddy KA, Katsuragi H (2017) Obstacle-shape effect in a two-dimensional granular silo flow field. Phys Rev Fluids 2:094302

Evesque P, Meftah W (1993) Mean flow of a vertically vibrated hourglass. Int J Mod Phys B 7(09n10):1799–1805

Garcimartín A, Zuriguel I, Pugnaloni LA, Janda A (2010) Shape of jamming arches in two-dimensional deposits of granular materials. Phys Rev E 82:031306

Gella D, Maza D, Zuriguel I, Ashour A, Arévalo R, Stannarius R (2017) Linking bottleneck clogging with flow kinematics in granular materials: the role of silo width. Phys Rev Fluids 2:084304

Gella D, Zuriguel I, Maza D (2018) Decoupling geometrical and kinematic contributions to the silo clogging process. Phys Rev Lett 121:138001

Goldberg E, Carlevaro CM, Pugnaloni LA (2018) Clogging in two-dimensions: effect of particle shape. J Stat Mech: Theory Exp 2018(11):113201

Guariguata A, Pascall MA, Gilmer MW, Sum AK, Sloan ED, Koh CA, Wu DT (2012) Jamming of particles in a two-dimensional fluid-driven flow. Phys Rev E 86:061311

Guerrero BV, Pugnaloni LA, Lozano C, Zuriguel I, Garcimartín A (2018) Slow relaxation dynamics of clogs in a vibrated granular silo. Phys Rev E 97:042904

Guerrero BV, Chakraborty B, Zuriguel I, Garcimartín A (2019) Nonergodicity in silo unclogging: broken and unbroken arches. Phys Rev E 100:032901

Hadjigeorgiou J, Stacey T (2013) The absence of strategy in orepass planning, design, and management. J South Afr Inst Min Metall 113:795–801

Helbing D, Johansson A, Mathiesen J, Jensen MH, Hansen A (2006) Analytical approach to continuous and intermittent bottleneck flows. Phys Rev Lett 97(16):168001

Hidalgo RC, Lozano C, Zuriguel I, Garcimartín A (2013) Force analysis of clogging arches in a silo. Granul Matter 15(6):841–848

Hong X, Kohne M, Morrell M, Wang H, Weeks ER (2017) Clogging of soft particles in two-dimensional hoppers. Phys Rev E 96:062605

Hou M, Chen W, Zhang T, Lu K, Chan C (2003) Global nature of dilute-to-dense transition of granular flows in a 2d channel. Phys Rev Lett 91(20):204301

Janda A, Zuriguel I, Garcimartín A, Pugnaloni LA, Maza D (2008) Jamming and critical outlet size in the discharge of a two-dimensional silo. EPL (Europhys Lett) 84(4):44002

Janda A, Harich R, Zuriguel I, Maza D, Cixous P, Garcimartín A (2009a) Flow-rate fluctuations in the outpouring of grains from a twodimensional silo. Phys Rev E 79:031302

Janda A, Maza D, Garcimartín A, Kolb E, Lanuza J, Clément E (2009b) Unjamming a granular hopper by vibration. EPL (Europhys Lett) 87(2):24002

Janda A, Zuriguel I, Garcimartín A, Maza D (2015) Clogging of granular materials in narrow vertical pipes discharged at constant velocity. Granul Matter 17(5):545–551

Janssen HA (1895) Versuche uber getreidedruck in silozellen. Z Ver Dtsch Ing 39(35):1045–1049

Jenike AW (1964) Steady gravity flow of frictional-cohesive solids in converging channels. J Appl Mech 31(1):5–11

Kamath S, Kunte A, Doshi P, Orpe AV (2014) Flow of granular matter in a silo with multiple exit orifices: jamming to mixing. Phys Rev E 90(6):062206

Kohring G, Melin S, Puhl H, Tillemans H, Vermöhlen W (1995) Computer simulations of critical, non-stationary granular flow through a hopper. Comput Methods Appl Mech Eng 124(3):273–281

Koivisto J, Durian DJ (2017) Effect of interstitial fluid on the fraction of flow microstates that precede clogging in granular hoppers. Phys Rev E 95:032904

Kondic L (2014) Simulations of two dimensional hopper flow. Granul Matter 16(2):235–242

Kramers HA (1940) Brownian motion in a field of force and the diffusion model of chemical reactions. Physica 7(4):284–304

Kunte A, Doshi P, Orpe AV (2014) Spontaneous jamming and unjamming in a hopper with multiple exit orifices. Phys Rev E 90:020201

Lafond PG, Gilmer MW, Koh CA, Sloan ED, Wu DT, Sum AK (2013) Orifice jamming of fluid-driven granular flow. Phys Rev E 87:042204

Liu AJ, Nagel SR (1998) Nonlinear dynamics: jamming is not just cool any more. Nature 396(6706):21

Longhi E, Easwar N, Menon N (2002) Large force fluctuations in a flowing granular medium. Phys Rev Lett 89:045501

Longjas A, Monterola C, Saloma C (2009) Force analysis of jamming with disks of different sizes in a two-dimensional hopper. J Stat Mech: Theory Exp 2009(05):P05006

López-Rodríguez D, Gella D, To, K, Maza D, Garcimartín A, Zuriguel I (2019) Effect of hopper angle on granular clogging. Phys Rev E 99:032901

Lozano C, Janda A, Garcimartín A, Maza D, Zuriguel I (2012a) Flow and clogging in a silo with an obstacle above the orifice. Phys Rev E 86:031306

Lozano C, Lumay G, Zuriguel I, Hidalgo RC, Garcimartín A (2012b) Breaking arches with vibrations: the role of defects. Phys Rev Lett 109:068001

Lozano C, Zuriguel I, Garcimartín A (2015) Stability of clogging arches in a silo submitted to vertical vibrations. Phys Rev E 91:062203

Mankoc C, Garcimartín A, Zuriguel I, Maza D, Pugnaloni LA (2009) Role of vibrations in the jamming and unjamming of grains discharging from a silo. Phys Rev E 80:011309

Marin A, Lhuissier H, Rossi M, Kähler CJ (2018) Clogging in constricted suspension flows. Phys Rev E 97:021102

Masuda T, Nishinari K, Schadschneider A (2014) Critical bottleneck size for jamless particle flows in two dimensions. Phys Rev Lett 112:138701

Merrigan C, Birwa SK, Tewari S, Chakraborty B (2018) Ergodicity breaking dynamics of arch collapse. Phys Rev E 97:040901

Mondal S, Sharma MM (2014) Role of flying buttresses in the jamming of granular matter through multiple rectangular outlets. Granul Matter 16(1):125–132

Mueth DM, Jaeger HM, Nagel SR (1998) Force distribution in a granular medium. Phys Rev E 57:3164–3169

Nguyen HT, Reichhardt C, Reichhardt CJO (2017) Clogging and jamming transitions in periodic obstacle arrays. Phys Rev E 95:030902

Nicodemi M, Coniglio A (1999) Aging in out-of-equilibrium dynamics of models for granular media. Phys Rev Lett 82(5):916

Nicolas A, Garcimartín Á, Zuriguel I (2018) Trap model for clogging and unclogging in granular hopper flows. Phys Rev Lett 120(19):198002

Pacheco-Martinez H, Van Gerner HJ, Ruiz-Suárez J (2008) Storage and discharge of a granular fluid. Phys Rev E 77(2):021303

Parretta A, Grillo P (2019) Flow dynamics of spherical grains through conical cardboard hoppers. Granul Matter 21(2):31

Pastor JM, Garcimartín A, Gago PA, Peralta JP, MartínGómez C, Ferrer LM, Maza D, Parisi DR, Pugnaloni LA, Zuriguel I (2015) Experimental proof of faster-is-slower in systems of frictional particles flowing through constrictions. Phys Rev E 92(6):062817

Patterson GA, Fierens PI, Sangiuliano Jimka F, König PG, Garcimartín A, Zuriguel I, Pugnaloni LA, Parisi DR (2017) Clogging transition of vibration-driven vehicles passing through constrictions. Phys Rev Lett 119:248301

Pérez G (2008) Numerical simulations in granular matter: the discharge of a 2d silo. Pramana 70(6):989–1007

Péter H, Libál A, Reichhardt C, Reichhardt CJ (2018) Crossover from jamming to clogging

behaviours in heterogeneous environments. Sci Rep 8(1):10252
Pournin L, Ramaioli M, Folly P, Liebling TM (2007) About the influence of friction and polydispersityon the jamming behavior of bead assemblies. Eur Phys J E 23(2):229
Pugnaloni LA, Valluzzi MG, Valluzzi LG (2006) Arching in tapped deposits of hard disks. Phys Rev E 73:051302
Roussel N, Nguyen TLH, Coussot P (2007) General probabilistic approach to the filtration process. Phys Rev Lett 98(11):114502
Sakaguohi H, Ozaki E, Igarashi T (1993) Plugging of the flow of granular materials during the discharge from a silo. Int J Mod Phys B 07(09n10):1949–1963
Saraf S, Franklin SV (2011) Power-law flow statistics in anisometric (wedge) hoppers. Phys Rev E 83:030301
Serrano DA, Cabrera D, Gutiérrez GJ, Medina A (2014) Experimental study of mass flow rate in a Silo under the wall width influence. Springer International Publishing, Cham, pp 207–217
Sheldon HG, Durian DJ (Dec 2010) Granular discharge and clogging for tilted hoppers. Granul Matter 12(6):579–585
Stoop RL, Tierno P (2018) Clogging and jamming of colloidal monolayers driven across disordered landscapes. Commun Phys 1(1):68
Suzuki A, Takahashi H, Tanaka T (1968) Behaviour of a particle bed in the field of vibration ii flow of particles through slits in the bottom of a vibrating vessel. Powder Technol 2(2):72–77
Tang J, Behringer RP (2016) Orientation, flow, and clogging in a two-dimensional hopper: Ellipses vs. disks. EPL (Europhys Lett) 114(3):34002
Tejada I, Sibille L, Chareyre B (2016) Role of blockages in particle transport through homogeneous granular assemblies. EPL (Europhys Lett) 115(5):54005
Tewari S, Dichter M, Chakraborty B (2013) Signatures of incipient jamming in collisional hopper flows. Soft Matter 9:5016–5024
Thomas CC, Durian DJ (2013) Geometry dependence of the clogging transition in tilted hoppers. Phys Rev E 87:052201
Thomas CC, Durian DJ (Apr 2015) Fraction of clogging configurations sampled by granular hopper flow. Phys Rev Lett 114:178001
Thomas CC, Durian DJ (2016) Intermittency and velocity fluctuations in hopper flows prone to clogging. Phys Rev E 94:022901
To K (2005) Jamming transition in two-dimensional hoppers and silos. Phys Rev E 71:060301
To K, Tai H-T (2017) Flow and clog in a silo with oscillating exit. Phys Rev E 96(3):032906
To K, Lai P-Y, Pak HK (2001) Jamming of granular flow in a two dimensional hopper. Phys Rev Lett 86:71–74
To K, Yen Y, Mo Y-K, Huang J-R (2019) Granular flow from silos with rotating orifice. Phys Rev E 100(1):012906
Uñac RO, Vidales AM, Pugnaloni LA (2012) The effect of the packing fraction on the jamming of granular flow through small apertures. J Stat Mech: Theory Exp 2012(04):P04008
Valdes JR, Santamarina JC (2008) Clogging: bridge formation and vibration-based destabilization. Can Geotech J 45(2):177–184
Vamsi Krishna Reddy A, Kumar S, Anki Reddy K, Talbot J (2018) Granular silo flow of inelastic dumbbells: clogging and its reduction. Phys Rev E 98:022904
Verbücheln F, Parteli EJR, Pösohel T (2015) Helical inner-wall texture prevents jamming in granular pipe flows. Soft Matter 11:4295–4305
Walker D (1966) An approximate theory for pressures and arching in hoppers. Chem Eng Sci 21(11):975–997
Wassgren CR, Hunt ML, Freese P, Palamara J, Brennen C (2002) Effects of vertical vibration on hopper flows of granular material. Phys Fluids 14(10):3439–3448
Wes G, Stemerding S, van Zuiliohem D (1990) Control of flow of cohesive powders by means of simultaneous aeration, and vibration. Powder Technol 61(1):39–49
Zhao Y, Cocco RA, Yang S, Chew JW (2019) Dem study on the effect of particle-size distribution on jamming in a 3d conical hopper. AICHE J 65(2):512–519
Zhou Y, Lagrée P-Y, Popinet S, Ruyer P, Aussillous P (2017) Experiments on, and discrete and continuum simulations of, the discharge of granular media from silos with a lateral orifice. J Fluid Mech 829:459–485
Zuriguel I, Pugnaloni LA, Garcimartín A, Maza D (2003) Jamming during the discharge of grains from a silo described as a percolating transition. Phys Rev E 68:030301
Zuriguel I, Garcimartín A, Maza D, Pugnaloni LA, Pastor JM (2005) Jamming during the discharge of granular matter from a silo. Phys Rev E 71:051303
Zuriguel I, Janda A, Garcimartín A, Lozano C, Arévalo R, Maza D (2011) Silo clogging reduction by the presence of an obstacle. Phys Rev Lett 107:278001
Zuriguel I, Parisi DR, Hidalgo RC, Lozano C, Janda A, Gago PA, Peralta JP, Ferrer LM, Pugnaloni LA, Clément E, Maza D, Pagonabarraga I, Garcimartín A (2014) Clogging transition of many-particle systems flowing through bottlenecks. Sci Rep 4:7324
Zuriguel I, Janda A, Arévalo R, Maza D, Garcimartín A (2017) Clogging and unclogging of many-particle systems passing through a bottleneck. EPJ Web Conf 140:01002